https://doi.org/10.1093/plcell/koac225 THE PLANT CELL 2022: 34: 4066–4087

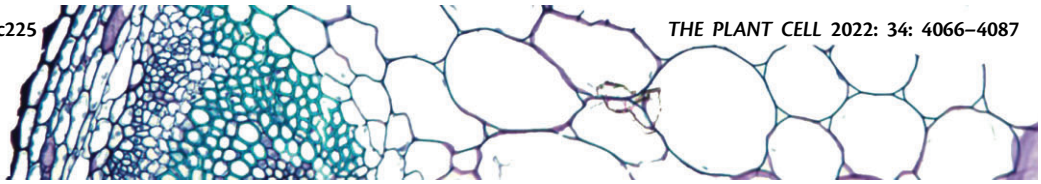

Research Article

The mycorrhiza-specific ammonium transporter ZmAMT3;1 mediates mycorrhiza-dependent nitrogen uptake in maize roots

Jing Hui ,[1] Xia An ,[1] Zhibo Li ,[1] Benjamin Neuhäuser ,[2] Uwe Ludewig ,[2] Xuna Wu ,[3] Waltraud X. Schulze ,[3] Fanjun Chen ,[1] Gu Feng ,[1] Hans Lambers ,[4] Fusuo Zhang [1] and Lixing Yuan [1,5,*]

1 College of Resources and Environmental Sciences, National Academy of Agriculture Green Development, Key Laboratory of Plant-Soil Interactions, MOE, China Agricultural University, Beijing, 100193, China
2 Department of Nutritional Crop Physiology, Institute of Crop Science, University of Hohenheim, Stuttgart, 70593, Germany
3 Department of Plant Systems Biology, Institute for Physiology and Biotechnology of Plants, University of Hohenheim, Stuttgart, 70593, Germany
4 School of Biological Science and Institute of Agriculture, University of Western Australia, Perth, WA6009, Australia
5 Center for Crop Functional Genomics and Molecular Breeding, China Agricultural University, Beijing, 100193, China

*Author for correspondence: yuanlixing@cau.edu.cn

L.Y. and J.H. designed the study and wrote the manuscript. J.H. performed experiments on transcriptome, gene expression, and biochemical analysis. X.A. and F. Chen constructed transgenic maize lines. J.H., Z.L., and X.A. performed the greenhouse and field experiments. W.S., X.W., and J.H. performed Phospho-proteomics. B.N., U.L., and J.H. performed oocytes experiment. L.Y., J.H., H.L., G.F., F.Z., W.S., B.N., and U.L. revised the manuscript.
The author responsible for distribution of materials integral to the findings presented in this article in accordance with the policy described in the instructions for Authors (https://academic.oup.com/plcell) is Lixing Yuan (yuanlixing@cau.edu.cn).

Abstract

Most plant species can form symbioses with arbuscular mycorrhizal fungi (AMFs), which may enhance the host plant's acquisition of soil nutrients. In contrast to phosphorus nutrition, the molecular mechanism of mycorrhizal nitrogen (N) uptake remains largely unknown, and its physiological relevance is unclear. Here, we identified a gene encoding an AMF-inducible ammonium transporter, *ZmAMT3;1*, in maize (*Zea mays*) roots. *ZmAMT3;1* was specifically expressed in arbuscule-containing cortical cells and the encoded protein was localized at the peri-arbuscular membrane. Functional analysis in yeast and *Xenopus* oocytes indicated that ZmAMT3;1 mediated high-affinity ammonium transport, with the substrate NH_4^+ being accessed, but likely translocating uncharged NH_3. Phosphorylation of ZmAMT3;1 at the C-terminus suppressed transport activity. Using *ZmAMT3;1-RNAi* transgenic maize lines grown in compartmented pot experiments, we demonstrated that substantial quantities of N were transferred from AMF to plants, and 68%–74% of this capacity was conferred by ZmAMT3;1. Under field conditions, the ZmAMT3;1-dependent mycorrhizal N pathway contributed $>30\%$ of postsilking N uptake. Furthermore, AMFs downregulated ZmAMT1;1a and ZmAMT1;3 protein abundance and transport activities expressed in the root epidermis, suggesting a trade-off between mycorrhizal and direct root N-uptake pathways. Taken together, our results provide a comprehensive understanding of mycorrhiza-dependent N uptake in maize and present a promising approach to improve N-acquisition efficiency via plant–microbe interactions.

Received February 10, 2022. Accepted June 18, 2022. Advance access publication July 26, 2022
© American Society of Plant Biologists 2022. All rights reserved. For permissions, please email: journals.permissions@oup.com

IN A NUTSHELL

Background: More than 80% of vascular plants can form symbiotic associations with arbuscular mycorrhizal fungi (AMFs). This ancient symbiosis evolved when plants conquered land, 400 million years ago, even before roots evolved. AMFs can greatly enhance the host plant's absorbing root surface for nutrient uptake. Within colonized roots, AMFs form tree-like structures (so-called arbuscules) in cortical cells, surrounded by a specialized host membrane, the peri-arbuscular membrane (PAM). Plant transporters reside in the PAM, mediating nutrient transfer from fungi to roots. As a major nitrogen (N) form, ammonium is somehow transported across the PAM. The discovery of the transport mechanism helps to elucidate mycorrhiza-dependent N (Myc-N) uptake in plants.

Question: To identify the PAM-localized ammonium transporters (AMTs) involved in the Myc pathway, we aimed to determine how important this route was for overall plant N nutrition.

Findings: We identified a mycorrhiza-inducible AMT gene, *ZmAMT3;1*, in roots of maize. The encoded protein was exclusively expressed at the PAM of the cortical cells that contain arbuscules and had high-affinity transport activity for ammonium. In the lab and in field experiments using *ZmAMT3;1-RNAi* transgenic maize plants, we determined that substantial amounts of N were transferred from the fungus to host plants via the transporter encoded by *ZmAMT3;1*. We demonstrated an essential role for ZmAMT3;1 in the Myc-N uptake and highlighted the physiological significance of AMF to overall plant N nutrition. This discovery provides a new avenue for improving crop N-use efficiency involving plant–microbe interactions.

Next steps: To enhance the sustainability of agriculture, we could engineer crops with greater Myc-N uptake by exploring superior/new alleles of *ZmAMT3;1* based on natural genetic variation or gene editing. We also made the fascinating discovery that AMFs may downregulate direct root N-uptake activity carried out by other AMTs in the root epidermis. Identification of upstream regulators coordinating Myc-N and root-N uptake pathways deserves further research.

Introduction

The symbiosis between plants and arbuscular mycorrhizal fungi (AMFs) is the most ubiquitous mutualistic association in plants. About 80%–90% of all terrestrial plants can form symbiotic associations with AMFs (Smith and Read, 2008). The establishment of AMF–plant interactions is based on the bidirectional transfer of nutrients at the plant–fungus interface between the symbiotic partners (Smith and Smith, 2012). In mycorrhizal associations, AMFs enhance mineral nutrient uptake of host plants, notably phosphorus (P) and nitrogen (N). In return, the host plants support AMFs with photosynthetically fixed carbon, mainly in the form of fatty acids (Bravo et al., 2017; Jiang et al., 2017; Keymer et al., 2017; Luginbuehl et al., 2017). Formation of an AMF symbiosis is considered a strategy evolved in plants to cope with nutrient deficiency, because external hyphae of AMFs access nutrients from a soil volume that is not accessible for roots and root hairs (Smith and Smith, 2011).

In addition to the direct N-uptake pathway via plant roots (Root-N pathway), numerous studies have suggested that AMFs transfer N to the host plants (Myc-N pathway) (Hodge et al., 2001; Govindarajulu et al., 2005; Leigh et al., 2009; Tian et al., 2010; Fellbaum et al., 2012; Bücking and Kafle, 2015; Chen et al., 2018; Makarov, 2019; Wang et al., 2020). Physiological and biochemical evidence indicates that extra-radical mycelia (ERMs) of AMFs take up inorganic (nitrate and ammonium) and organic (amino acids and small peptides) N sources from soil, and rapidly metabolize these into arginine (Arg) (Johansen et al., 1993; Tobar et al., 1994; Hawkins et al., 2000; Jin et al., 2005; Hodge and Fitter, 2010). The Arg in ERMs is then translocated to the intra-radical mycelia (IRMs) together with polyphosphate (PolyP) and catabolized into ammonium (NH_4^+/NH_3) that is subsequently released into the apoplast between the root and mycorrhizal fungi (Bago et al., 2001; Govindarajulu et al., 2005; Jin et al., 2005). The transport of ammonium across the peri-arbuscular membrane (PAM) is, therefore, expected to be crucial for mycorrhiza-dependent N (Myc-N) uptake (Chalot et al., 2006; Tian et al., 2010; Courty et al., 2015). A recent study also suggests that symbiotic nitrate uptake in rice (*Oryza sativa*) is conferred by the PAM-localized nitrate transporter OsNPF4.5 (Wang et al., 2020). Thus, the Myc-N pathway may result from the combined transfer of ammonium and nitrate across the PAM.

Many plant *AMT* genes are specifically induced by AMF, and their encoded proteins are localized at the PAM; such genes include *LjAMT2;2* in *Lotus japonicus* (Guether et al., 2009), *GmAMT4.1* in *Glycine max* (Kobae et al., 2010), *SbAMT3;1* and *SbAMT4;1* in *Sorghum bicolor* (Koegel et al., 2013), *MtAMT2;3* and *MtAMT2;4* in *Medicago truncatula* (Breuillin-Sessoms et al., 2015). These transporters are thought to mediate NH_3 or NH_4^+ transport at the symbiotic interface. However, *MtAMT2;3* does not transport ammonium, but instead acts as an ammonium sensor regulating the development of arbuscules and thereby affecting symbiotic nutrient (N and P) acquisition (Javot et al., 2011;

Breuillin-Sessoms et al., 2015). Thus, the nature of AMT-mediated ammonium transport across the PAM for Myc-N uptake remains largely unknown.

AMFs can transfer N to host plants, but the contribution of Myc-N uptake to overall plant N nutrition, particularly under field conditions, is still under debate (Smith et al., 2011; Smith and Smith, 2011; Bücking and Kafle, 2015; Makarov, 2019; Balestrini et al., 2020; Dellagi et al., 2020). Some argue that the increased N uptake in mycorrhizal plants is not a consequence of Myc-N uptake, but an effect of enhanced growth resulting from mycorrhiza-dependent P (Myc-P) uptake (Hamel and Smith, 1991; Corrêa et al., 2015). The contribution of Myc-N uptake may also be underestimated if the Root-N uptake pathway is downregulated, as shown for P uptake; in mycorrhizal plants the Root-P pathway is suppressed to the extent that this may even reduce the overall P uptake in some plants (Smith et al., 2004; Grace et al., 2009). Additionally, AMFs may compete for N with their host plants when soil N availability is very low, and thereby reduce beneficial effects or even inhibit plant growth (Hawkins and George, 1999; Reynolds et al., 2005; Püschel et al., 2016; Wang et al., 2018). The absence of mutants that are exclusively defective in ammonium transport at the symbiotic interface has restricted progress in efforts to quantify the physiological contributions of the Myc-N pathway to overall plant N nutrition.

In this study, using a transcriptome approach, we identified a mycorrhiza-inducible ammonium transporter (AMT) gene in maize (*Zea mays*), *ZmAMT3;1*, and found that the encoded protein was exclusively localized at the PAM. Heterologous expression in yeast and *Xenopus* oocytes showed that the ZmAMT3;1 protein-mediated high-affinity ammonium transport with NH_3 as substrate. We generated *ZmAMT3;1-RNAi* transgenic maize plants and quantified the phenotypic effect of ZmAMT3;1-dependent Myc-N uptake using pot experiments with a $^{15}N\text{-}NH_4^+$ patch or a separate NH_4^+-rich compartment to which only AM hyphae had access. A significant contribution of *ZmAMT3;1* to postsilking N uptake was further determined in 2 years of field experiments. Our study demonstrates an essential role for *ZmAMT3;1* in the Myc-N pathway and highlights the physiological relevance of AMFs to overall plant N nutrition, providing a novel avenue for improving crop N-use efficiency.

Results

Mycorrhiza-inducible expression of AMT ZmAMT3;1 in maize

Transcriptomic analysis of maize roots inoculated with or without AMFs revealed that several genes including AMTs and nitrate transporters were induced by AMFs (Figure 1A; Supplemental Figure S1). Among eight maize AMT genes, *ZmAMT3;1* was significantly induced by AMF inoculation, with a Log_2Fold-Change of 5.6 (Figure 1A). Using reverse transcription quantitative PCR (RT-qPCR; primers used are listed in Supplemental Table S1), we found that *ZmAMT3;1* was expressed in roots of field-grown maize plants, but not in roots of hydroponically grown plants that were unable to establish a symbiosis with AMFs (Figure 1B). In pot experiments, using different strains of AMF (*Rhizophagus intraradices* [*Ri*], *Glomus mosseae* [*Gm*], *Glomus versiforme* [*Gv*], a mixed culture of three strains [*Mix*]), increased the *ZmAMT3;1* transcript up to 100-fold in roots of maize (Figure 1C). In a time-course experiment from 14 to 42 days postinoculation (dpi) with AMFs, expression levels of *ZmAMT3;1* were significantly increased at 28 dpi, correlating with enhanced root length colonization (Figure 1, E and F). Following the developmental growth periods of plants, presumably along with increased AMF colonization (Schalamuk et al., 2004; Buade et al., 2020), *ZmAMT3;1* expression continuously increased in the mycorrhizal roots and reached maximum levels at the maturation stage (Figure 1G). Expression levels of the mycorrhizal root-specific maize phosphate transporter gene *ZmPht1;6*, a mycorrhiza-responsive gene marker (Glassop et al., 2005; Nagy et al., 2006), were consistent with changes of *ZmAMT3;1* expression under various treatments of AMF (Figure 1, D, F, and H).

ZmAMT3;1 is exclusively expressed in arbuscule-containing cells and the encoded protein localizes at the PAM

We used in situ hybridization to investigate the cellular location of the *ZmAMT3;1* transcript in mycorrhizal roots of maize at 42 dpi. Using high-stringency hybridization with the antisense probe, strong signals were detected in arbuscule-containing cortical cells (Figure 2A). In these colonized cells, however, no signal was detectable by hybridization with the sense probes (Figure 2B). The transgenic maize roots expressing the *ZmAMT3;1* promoter::GUS (β-glucosidase) fusion construct were further used to examine the cell specificity of *ZmAMT3;1* gene expression in mycorrhizal roots (Figure 2, C–E). By histochemical GUS staining in both cross sections and longitudinal sections of mycorrhizal roots, strong GUS activities were detected in the cortex of mycorrhizal roots (Figure 2, D and E). The root sections co-stained with WGA-488, a specific dye for AM fungal structures, further confirmed that *ZmAMT3;1* promoter-dependent GUS activities were expressed in the AMF-colonized cortical cells containing highly branched arbuscules, but not in cells containing only intracellular hyphae or cells without AMF colonization.

To determine subcellular localization, the ZmAMT3;1-GFP fusion protein was transiently expressed under the control of a *35S* promoter in maize mesophyll protoplasts (Figure 2F). In contrast with the cytosolic location of free GFP, the ZmAMT3;1-dependent green fluorescence was detected as a fine ring at the cell periphery that merged with red fluorescence from the plasma membrane-specific dye FM4-64, indicating localization at the plasma membrane. This plasma-membrane localization was further verified by expressing the ZmAMT3;1-GFP fusion protein in onion epidermal cells (Supplemental Figure S2). The ZmAMT3;1-GFP fusion protein was further expressed under control of its native promoter in transgenic maize plants (Figure 2G). In mycorrhizal roots, the

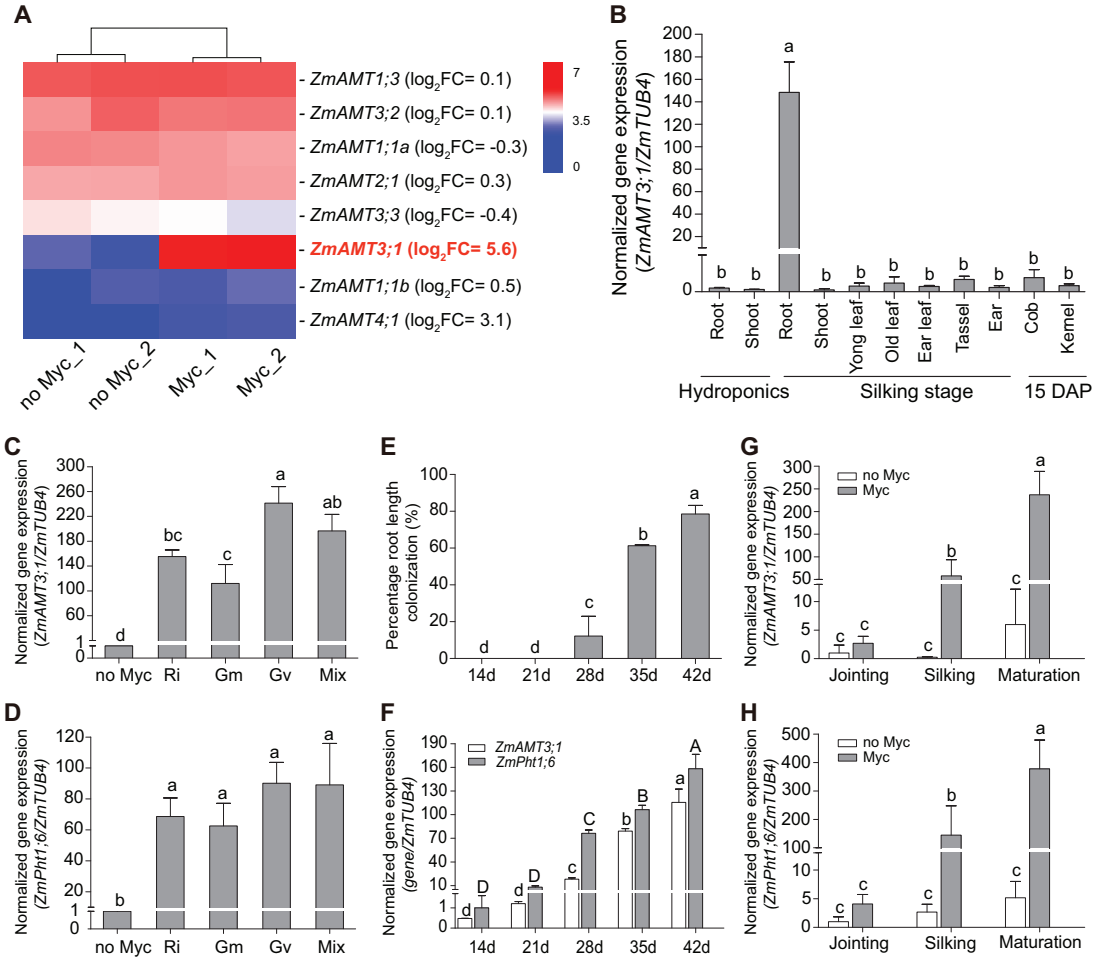

Figure 1 Mycorrhiza-inducible expression of AMT *ZmAMT3;1* in maize roots. A, Heatmap analysis of *ZmAMT* gene expression by an RNA-seq approach. Log_2-fold differences in gene expression levels were used to create the heatmap. B, Normalized expression of *ZmAMT3;1* in different organs of hydroponically- and field-grown maize plants. The values are the means of 3–4 biological replicates, and error bars represent SD. *ZmTUB4* was used as the reference transcript. Relative gene expression was normalized by that in roots grown hydroponically. DAP, days after pollination. C and D, Normalized expression of *ZmAMT3;1* (C) and *ZmPht1;6* (D) in maize roots inoculated with different AMF strains. The values are the means of 3–4 biological replicates, and error bars represent SD. *ZmTUB4* was used as the reference transcript. Relative gene expression was normalized by that of no Myc. E and F, Quantification of root colonization rate (E), and the normalized expression of *ZmAMT3;1* and *ZmPht1;6* (F) in *Ri* strain inoculated roots of maize plants at 14, 21, 28, 35, and 42 days post inoculation (dpi). The values are the means of 3–4 biological replicates, and error bars represent SD. *ZmTUB4* was used as the reference transcript. Relative gene expression was normalized by that in roots grown at 14 dpi. G and H, Normalized expression of *ZmAMT3;1* (G) and *ZmPht1;6* (H) in *Ri* inoculated (Myc) and noninoculated (no Myc) roots of maize plants harvested at different development stages. The values are the means of 3–4 biological replicates, and error bars represent SD. *ZmTUB4* was used as the reference transcript. Relative gene expression was normalized by that in roots grown at jointing stage. One-way ANOVAs (Duncan's *F*-test) were performed, and different letters indicate significant differences ($P < 0.05$).

ZmAMT3;1-GFP signal was exclusively detected in arbuscular cortical cells. Strong GFP signals were observed at the periphery of arbuscular branches, suggesting a PAM localization. In contrast, no GFP signal was found on the plasma membranes of cortical cells in inoculated roots. Taken together, these results indicate that *ZmAMT3;1* was exclusively expressed in arbuscular cortical cells, and the encoded protein was localized at the PAM of arbuscule branches.

ZmAMT3;1 mediates high-affinity ammonium transport in yeast and transports NH_3 in oocytes

Functionality of ZmAMT3;1 was verified by heterologous expression in the yeast triple-Δ*mep* (*1–3*) mutant (*31,019b*) that is defective in high-affinity ammonium uptake (Marini et al., 1997). Expression of *ZmAMT3;1* restored the growth of the yeast mutant with supplies of 0.5–10 mM NH_4^+ as sole N source (pH 5.5) (Figure 3A). Expression of the rice orthologous gene *OsAMT3:1* in yeast, however, did not confer any ammonium transport capacity (Supplemental Figure S3). Growth promotion of yeast strains expressing LjAMT2;2 (AMT2-type AMT in *L. japonicus*) and NeRh (Rhesus-type ammonia transporter in *Nitrosomonas europaea*) was pH dependent with better growth at acidic pH (pH < 5.5) or alkaline pH (pH > 6.5), respectively, as observed in previous studies (Weidinger et al., 2007; Guether et al., 2009). In contrast, growth complementation by

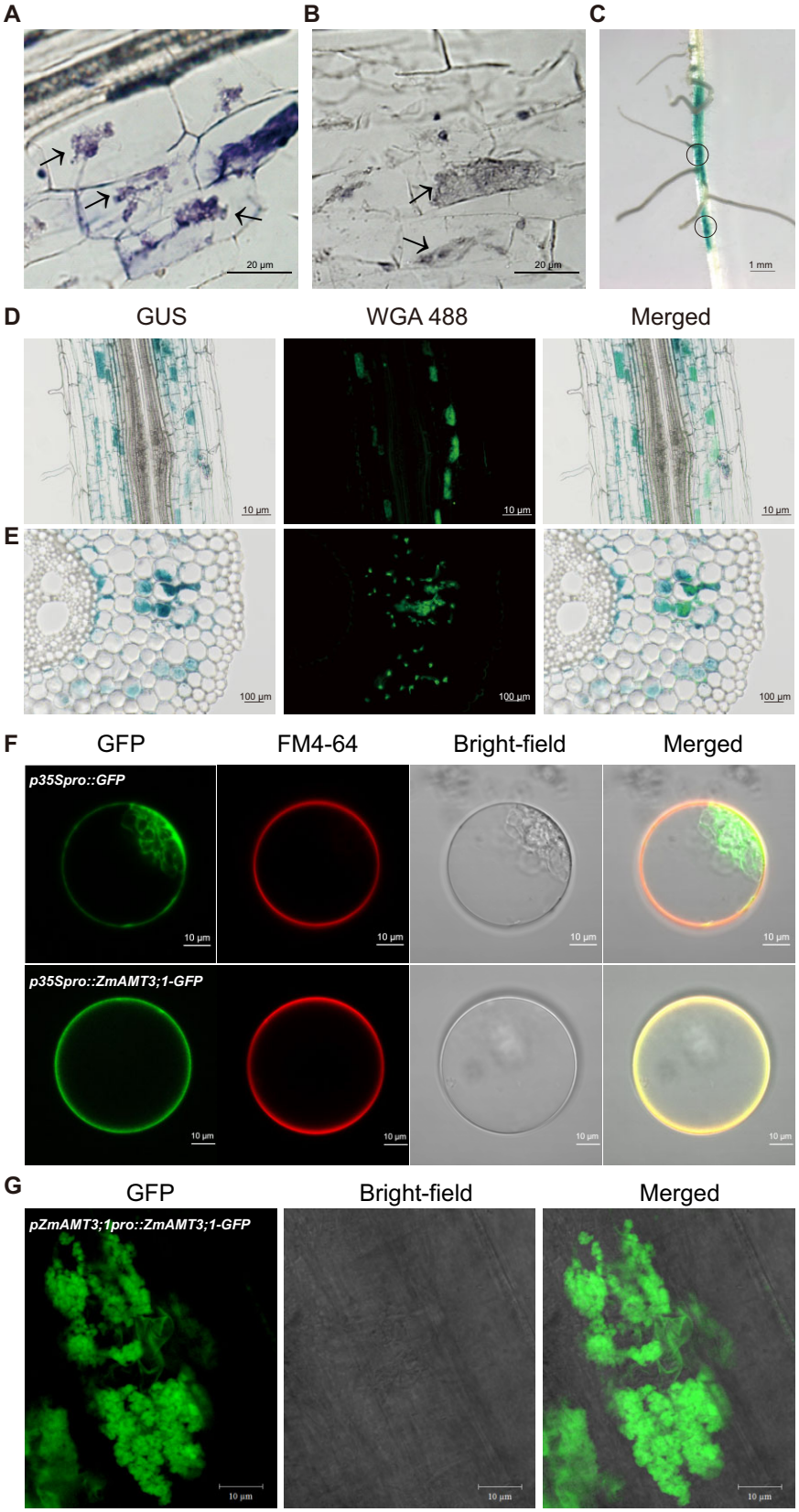

Figure 2 Arbuscular cortical cell-specific expression and PAM localization of ZmAMT3;1 in maize roots. A and B, In situ hybridization in mycorrhized root sections hybridized with the *ZmAMT3;1* antisense (A) or sense (B) probe, respectively. The antisense probes hybridized (dark purple) only to plant cells containing arbuscules. Black arrows indicate arbuscule. Scale bars = 20 μm. C, GUS staining in primary and lateral roots of transgenic maize plants inoculated by AMF. Scale bars = 1 mm. D, Longitudinal section and cross section (E) of transgenic maize roots expressing GUS co-staining with wheat germ agglutinin Alexa Fluor (WGA-488), which was used to visualize the fungal structures. Scale bars = 10 μm (D), 100 μm

(continued)

ZmAMT3;1, like that of AtAMT2;1, did not change with pH (Figure 3A; Sohlenkamp et al., 2002). A ^{15}N-labeled ammonium influx assay in yeast was further conducted to assess kinetic properties of ZmAMT3;1 when the external $^{15}NH_4^+$ concentrations ranged from 10 to 500 μM (Figure 3B). By calculating the net ammonium-uptake rates mediated by ZmAMT3;1, the resulting saturable curve fit well with the Michaelis–Menten equation and yielded a K_m value of 16.6 ± 3.4 μM and a V_{max} value of 0.29 ± 0.01 μmol μg^{-1} cells min^{-1}. These results indicate that *ZmAMT3;1* encoded a functional high-affinity AMT in yeast.

In yeast, the ZmAMT3;1 activity was independent of the external pH, indicating that the transporter recruited NH_4^+, rather than NH_3, since at a certain ammonium concentration, the NH_4^+ concentration is fairly constant between pH 3.5 and pH 7, while the NH_3 concentration declines 10-fold per pH unit. To determine the transporter characteristics of ZmAMT3;1, it was heterologously expressed in oocytes (Figure 3, C–F). First, the plasma membrane localization of ZmAMT3;1 was confirmed by expressing the ZmAMT3;1-GFP fusion protein in cells of oocytes (Figure 3C). Second, the oocytes were used for a ^{15}N-labeled ammonium uptake assay, and ZmAMT3;1-injected oocytes revealed significantly greater accumulation of ^{15}N than the control (Figure 3D), indicating that ZmAMT3;1 was also functional in *Xenopus* oocytes. The ZmAMT3;1-mediated net $^{15}NH_4^+$ uptake was further shown to be independent of external pH, confirming that the transporter recruited NH_4^+ (Supplemental Figure S4). When the oocytes were subjected to an electrophysiological assay, the ZmAMT3;1-expressing oocytes did not exhibit a change in inward current under NH_4^+ supply, similar to cells without injection (NI) (Figure 3, E and F). As previously reported, the oocytes expressing AtAMT1;2 caused a large ammonium-dependent inward current associated with electrogenic ammonium transport (Neuhäuser et al., 2007). Ammonium transport was thus not associated with ionic currents, suggesting that ZmAMT3;1 likely transported uncharged NH_3, rather than ionic NH_4^+.

Transport activity of ZmAMT3;1 is regulated by C-terminus phosphorylation

The AMT family comprises the AMT1- and AMT2-subfamilies, and the latter is further split into three clusters: AMT2, AMT3, and AMT4 (Koegel et al., 2013, 2017). A phylogenetic analysis of protein sequences showed that AMT3-cluster members in grass species include three subclusters: AMT3;1, AMT3;2, and AMT3;3 (Figure 4A). Those members within the AMT3;1 subcluster all revealed mycorrhiza-inducible expression patterns, which suggests they share a common ancestor (Koegel et al., 2017). Plant AMT1-type transporter activities can be posttranslationally inhibited via phosphorylation of their cytosolic C-terminus region (CTR) (Loqué et al., 2007; Neuhäuser et al., 2007; Lanquar et al., 2009; Yuan et al., 2013; Wu et al., 2019a). CTR sequence alignment of AMT3-cluster members revealed three conserved putative phosphorylation sites, equivalent to ZmAMT3;1 T465, S471, and T485 (Figure 4A). Three additional putative phosphorylation sites (corresponding to ZmAMT3;1 S464, T475, and S482) were exclusively conserved within the AMT3:1-subcluster.

To explore whether the putative phosphorylation sites are involved in regulating ZmAMT3;1 transporter activity, mutants mimicking the constitutive phosphorylation (S/T substituted by D) or de-phosphorylation state (S/T substituted by A) were functionally expressed in the yeast mutant *31019b* (Figure 4B; Supplemental Figure S5). Yeast expressing ZmAMT3;1 S464D, T475D, or S482D phosphor-mutants, mimicking phosphorylation of AMT3;1-subcluster-conserved sites, showed a reduced growth complementation compared with those of wild-type (WT) or mutants mimicking the de-phosphorylation form (S464A, T475A, or S482A) at different levels of external ammonium supply or pH. In contrast, no growth difference was detected between yeast cells expressing the ZmAMT3;1 WT and phosphor-mutants corresponding to AMT3-cluster conserved sites (S471D and T485D), except for a growth depression of T465D which might have resulted from interplay of the adjacent site S464. Similar to ZmAMT3;1-expressing oocytes, those cells with the phospho-mutants did not exhibit a change in inward current under NH_4^+ supply (Supplemental Figure S6). The oocytes expressing ZmAMT3;1 phosphor-mimicking mutants T475D or S482D, but not S471D and T485D, revealed reduced ^{15}N-labeled ammonium accumulation compared with those expressing the WT or corresponding de-phosphor-mutants (Figure 4C). These results indicate that ZmAMT3;1 transporter activity could be downregulated by phosphorylation of those sites that were exclusively conserved among AMT3;1-subcluster members.

Root epidermis-expressed *ZmAMT1s* are downregulated at the protein level by AMFs

The relationships between the Root-N and Myc-N pathways in maize were investigated by quantitatively comparing expression of overall *ZmAMT* genes at transcript and protein levels by RT-qPCR and proteomics, respectively (Figure 5). In mycorrhizal roots of maize at 42 dpi, transcript and protein abundance of ZmAMT3;1 increased up to ∼100-fold and ∼60-fold, respectively, compared with nonmycorrhizal roots (Figure 5, A and B). Although *ZmAMT4;1* was

Figure 2 (Continued)

(E). F, Plasma-membrane localization of ZmAMT3;1 in maize mesophyll protoplasts. Maize mesophyll protoplasts transiently expressing free GFP or ZmAMT3;1-GFP fusion proteins were dyed with a plasma membrane-specific dye FM4–64 and imaged using confocal microscopy. Scale bars = 10 μm. G, Confocal laser scanning images of transgenic maize roots, transformed with the *pZmAMT3;1pro::ZmAMT3;1-GFP* plasmid. Bright-field: bright-field images; Merged: merged fluorescent images. Scale bars = 10 μm.

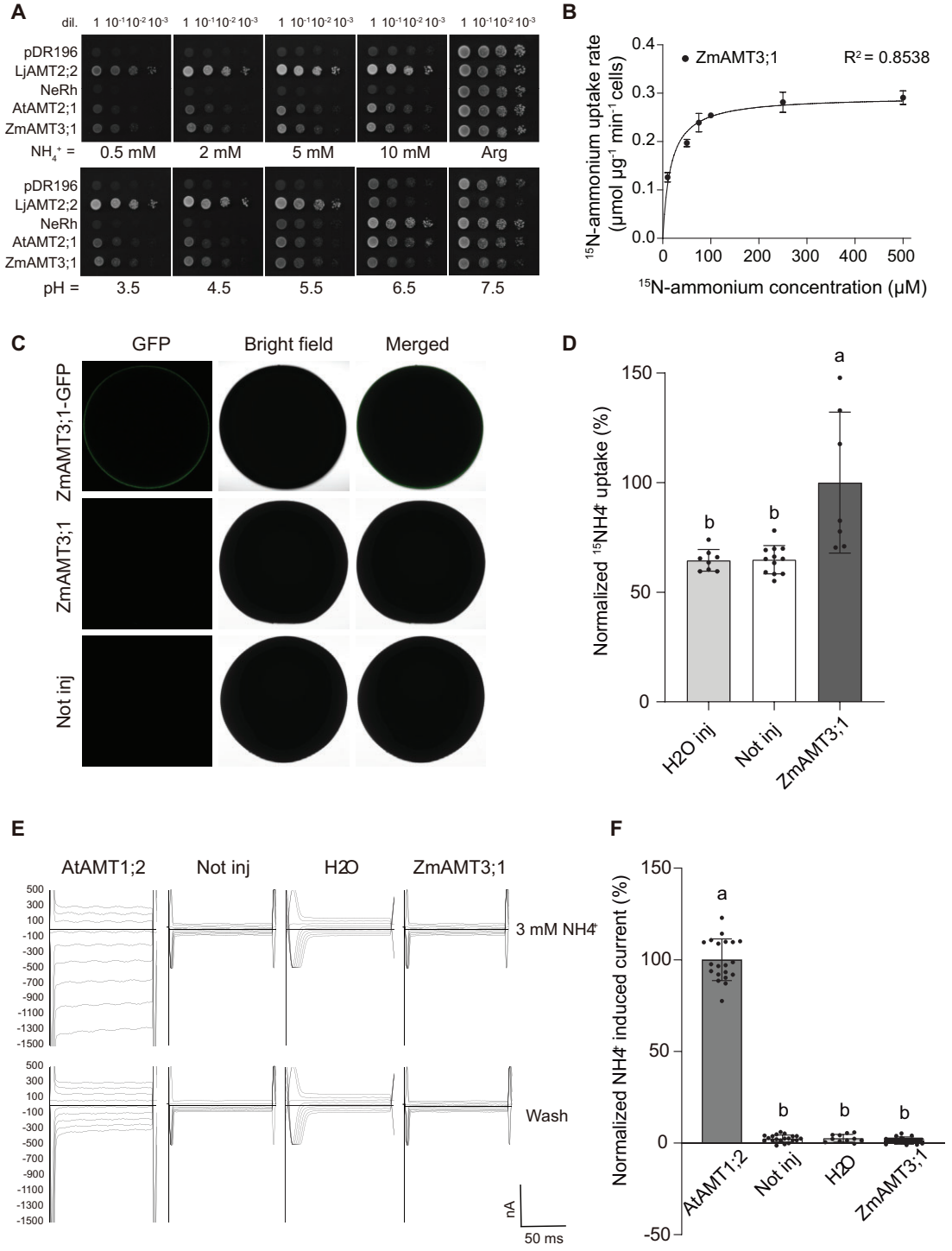

Figure 3 Ammonium transport of ZmAMT3;1 in yeast and oocytes. A, Functional complementation of *ZmAMT3;1* in ammonium uptake-defective yeast strain *31,019b* (ΔΔΔ*mep1;2;3*). Yeast cells were transformed with *ZmAMT3;1*, *AtAMT2;1*, *LjAMT2;2*, *NeRh* and the empty vector *pDR196*. Dilutions of the transformants were grown on YNB plates supplemented with indicated concentrations of NH_4^+ or Arg as sole N source at pH 3.5, or 2 mM ammonium at indicated pH levels for 4 days at 28°C. B, Kinetic analysis of ZmAMT3;1 in ammonium uptake. ^{15}N-labeled ammonium influx mediated by ZmAMT3;1 was calculated by subtracting the value of pDR196-expressing yeast from ZmAMT3;1-expressing yeast. Curves were fitted using the Michaelis–Menten equation, yielding K_m = 16.6 ± 3.4 μM and V_{max} = 0.29 ± 0.01 μmol μg^{-1} cells min^{-1}. C, Membrane localization of ZmAMT3;1-GFP in *Xenopus laevis* oocytes. Confocal laser scanning images of oocytes expressing ZmAMT3;1-GFP fusion protein, ZmAMT3;1 or noninjected oocytes. D, Normalized ^{15}N-labelled ammonium accumulation from oocytes injected with ZmAMT3;1, water injected or not injected controls. Data are means ± SD (n = 7∼12, biological replicates). Different lowercase letters indicate significant differences by one-way ANOVA (Duncan's F-test, $P < 0.01$). E, The ZmAMT3;1- and AtAMT1;2-dependent current measured in *Xenopus* oocytes. Original traces of ionic currents were taken for 50 ms starting at 40 mV declining in steps of 20 mV to −120 mV. Oocytes expressing ZmAMT3;1, AtAMT1;2, water-injected or noninjected oocytes in the presence of ammonium (3 mM, upper panels) and in the absence of ammonium (wash, lower panels). Axis indicates

(continued)

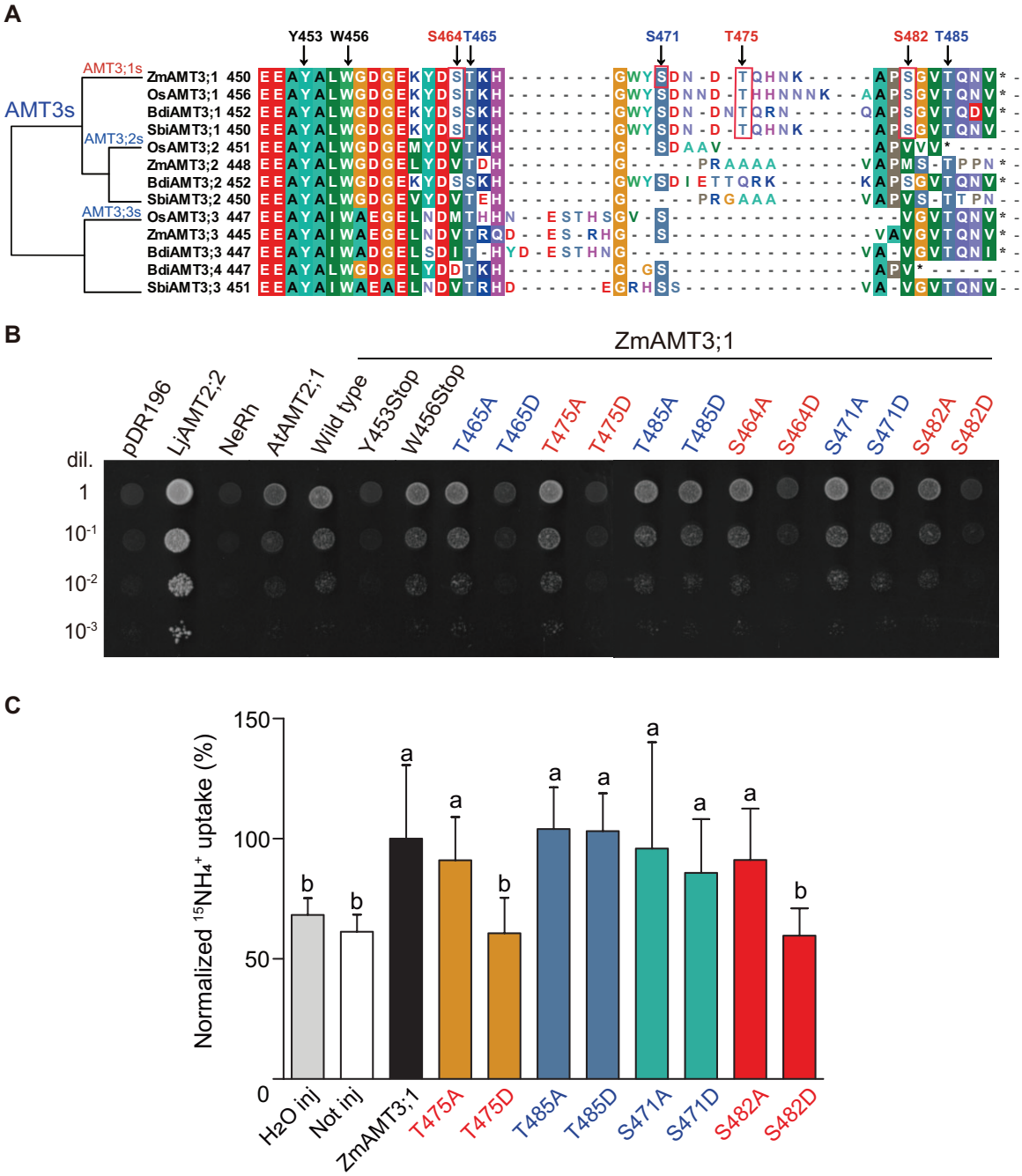

Figure 4 Functional characterization of phospho-mutants of ZmAMT3;1 in yeast and oocytes. A, Alignment of AMT3s members with deduced amino acid sequences of conserved CTR. Phosphorylation sites are indicated by *downward arrow*. B, Ammonium transport activity of ZmAMT3;1 regulated by phosphorylation of CTR. The yeast strain *31,019b* was transformed with plasmid *pDR196*, *AtAMT2;1*, *LjAMT2;2*, *NeRh*, *ZmAMT3;1*, *ZmAMT3;1* CTR-deletion mutants (*Y453Stop* and *W456Stop*) and *ZmAMT3;1* phospho-mutants (*T465A*, *T465D*, *T475A*, *T475D*, *T485A*, *T485D*, *S464A*, *S464D*, *S471A*, *S471D*, *S482A*, and *S482D*). Dilutions of the transformants were grown on YNB plates supplemented with 2 mM ammonium as the sole nitrogen (N) source at pH 3.5 for 4 days at 28°C. C, Functional analysis of phospho-mutants of ZmAMT3;1 in *X. laevis* oocytes. Normalized ^{15}N-ammonium uptake from three independent experiments from oocytes injected with *ZmAMT3;1*, phospho-mutants (*T475A*, *T475D*, *T485A*, *T485D*, *S471A*, *S471D*, *S482A*, and *S482D*), water-injected or noninjected controls. Data are means ± SD (n = 3–9, biological replicates). Different lowercase letters indicate significant differences by one-way ANOVA (Duncan's F-test, $P < 0.01$).

Figure 3 (Continued)
current in nanoampere. F, The inward currents by 3 mM NH_4Cl at a membrane potential of −100 mV from oocytes injected with AtAMT1;2, ZmAMT3;1, water-injected or noninjected oocytes. Data are means ± SD (n = 11–20, biological replicates). Different lowercase letters indicate significant differences by one-way ANOVA (Duncan's F-test, $P < 0.01$).

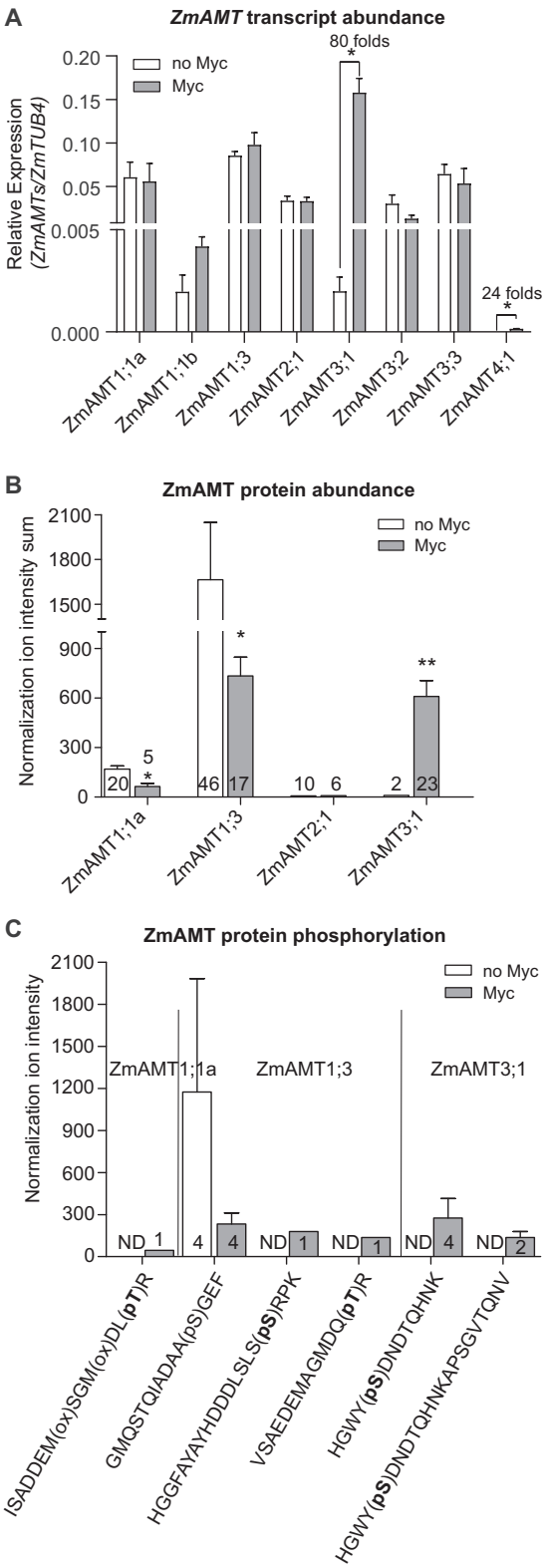

Figure 5 Regulation of ZmAMTs in AMF-inoculated maize roots. A, Relative expression of *ZmAMTs* was quantified in mycorrhizal (Myc) and nonmycorrhizal roots (no Myc) by quantitative real-time PCR. *ZmTUB4* was used as the reference transcript. Bars indicate means ± SD (n = 3, biological replicates). Asterisks indicate significant differences between Myc and no Myc treatments by t test ($^{*}P < 0.05$). Numbers above the column indicate induction degree of gene expression by Myc treatments. B, ZmAMTs protein abundance in the same organ as (A) were quantified by proteomics. Ion intensity sums of identified peptides of different ZmAMTs are shown as averages with standard deviations from three independent root samples. Numbers indicate the total of spectra acquired for peptides identifying each of the respective ZmAMTs. Numbers indicate the total of spectra acquired for peptides identifying each of the respective ZmAMTs. Asterisks indicate significant differences between Myc and no Myc treatments by t test ($^{*}P < 0.05$; $^{**}P < 0.01$). C, Normalized ion intensity of ZmAMTs phosphopeptides identified from phosphor-proteomics. Bars represent averaged normalized ion intensities with standard deviations from three independent root preparations. Numbers indicate the total number of spectra acquired for each of the phosphopeptides. ND, not determined.

also upregulated transcriptionally by AMFs, the transcript abundance was very low, and no corresponding peptide was detected (Figure 5, A and B). Two root epidermis-expressed AMT1-type AMTs, *ZmAMT1;1a* and *ZmAMT1;3*, mediate NH_4^+ uptake, representing the major components of the Root-N pathway for ammonium uptake in maize (Gu et al., 2013). After mycorrhizal inoculation, the transcripts of *ZmAMT1;1a* and *ZmAMT1;3* were unchanged (Figure 5A), but, interestingly, the abundances of ZmAMT1;1a and ZmAMT1;3 proteins were significantly downregulated to half their levels (Figure 5B).

As revealed by the phosphor-proteomic analysis, mycorrhiza-inducible phosphorylation modifications were detected at T452 for ZmAMT1;1a, and T452 and S470 for ZmAMT1;3 (Figure 5C; Supplemental Figure S7). Phosphorylation of the T452 residue at ZmAMT1;1a or ZmAMT1;3 downregulates the transporter activity, similar to the two equivalent sites (AtAMT1;1 T460/AtAMT1;3 T464) in roots of Arabidopsis (Loqué et al., 2007; Yuan et al., 2013; Hao et al., 2020). Under mycorrhizal inoculation, however, most of the putative phosphor-sites of ZmAMT3;1 were not detected, suggesting dominance of dephosphorylation status of ZmAMT3;1 as an active state of the transporters (Figures 4, B and C and 5C; Supplemental Figure S7). The S471 phosphor-modification was enhanced in the presence of AMF, probably owing to an apparent effect of a general increase in protein abundance, but it did not inhibit transporter activity of ZmAMT3;1. These results indicate that AMF colonization upregulated ZmAMT3;1 transcript and protein levels, thus inducing the Myc-N pathway, while downregulating the epidermis-expressed ZmAMTs at translational and posttranslational levels, thereby repressing the Root-N pathway.

ZmAMT3;1 mediated ^{15}N transfer from AMF to host plants

To investigate the role of *ZmAMT3;1* in transferring N from AMF to host plants, transgenic maize lines with downregulated *ZmAMT3;1* transcripts were generated by an RNA-mediated interference (RNAi)-based silencing

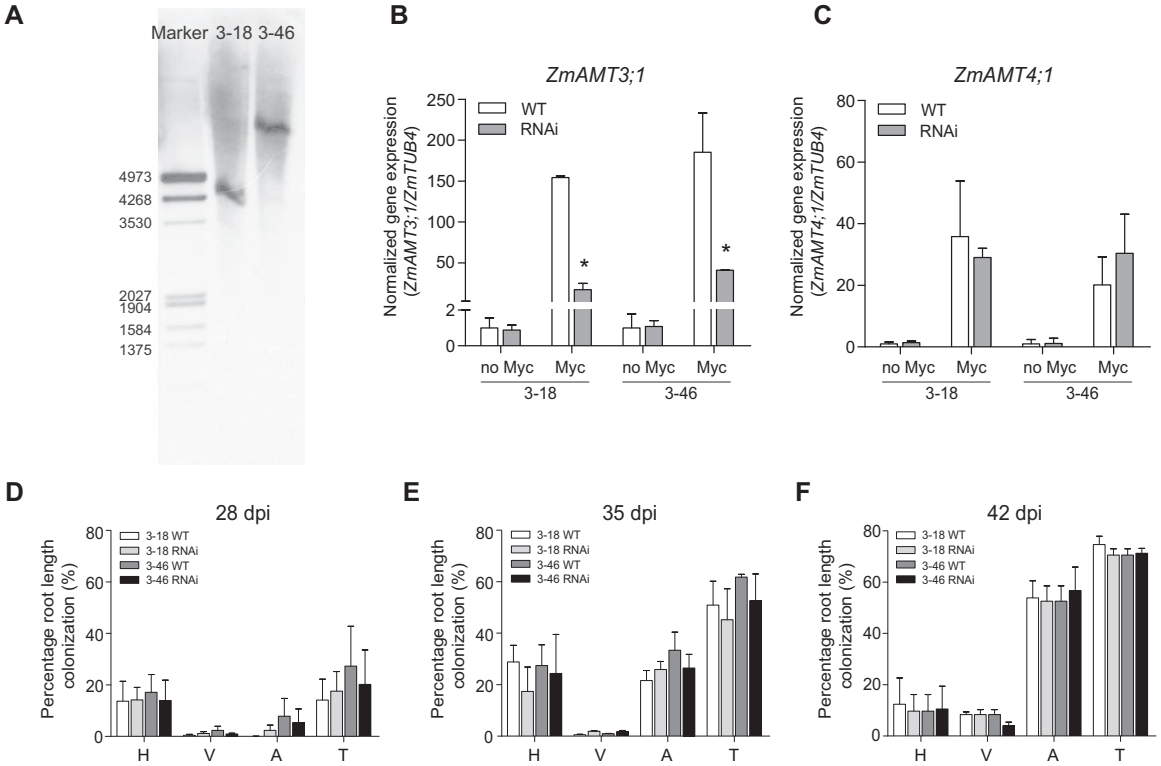

Figure 6 Silencing *ZmAMT3;1* gene did not affect mycorrhizal symbiosis. A, DNA gel blot analysis of transgenic maize lines. Genomic DNA was digested with restriction enzyme *Hind* III. Blots were probed with full length of bar gene at high stringency. Numbers on the left indicate length of DNA fractions revealed by molecular weight markers. *3–18* and *3–46* represented two independent RNAi lines. B and C, Normalized expression of the *ZmAMT3;1* (B) and *ZmAMT4;1* (C) gene in the mycorrhizal (Myc) and nonmycorrhizal roots (no Myc) of WT and two independent RNAi lines *3–18* and *3–46* at 42 dpi. Bars indicate means ± SD (n = 4, biological replicates). *ZmTUB4* was used as the reference transcript. Relative gene expression of each line was normalized by that in no Myc. Asterisks indicate significantly different means (Student's t test, $^{*}P < 0.05$). D–F, Quantification of root colonization rate in mycorrhizal roots of maize plants at 28 (D), 35 (E), and 42 (F) dpi. Bars indicate means ± SD (n = 3, biological replicates). H, hyphae. V, vesicles. A, arbuscular cells. T, total AMF colonization rate.

approach. Two independent, single-copy transgenic events (*3–18* and *3–46*) were identified by DNA gel blot analysis and backcrossed with WT line B73 (Figure 6A). In mycorrhizal roots of maize at 42 dpi, transcripts of *ZmAMT3;1* in both RNAi lines were significantly reduced, to 11%–22% of those in WT (Figure 6B). Transcripts of other *ZmAMTs* including close homologs in the *AMT3-subcluster* (*ZmAMT3;2* and *ZmAMT3;3*) were unaffected in mycorrhizal roots of RNAi lines, suggesting specific suppression of *ZmAMT3;1* (Figure 6C; Supplemental Figure S8). Meanwhile, expression levels of Myc-specific *ZmNPF4.5* and *ZmPht1;6* were not affected by silencing of *ZmAMT3;1* (Supplemental Figure S9). To determine whether *ZmAMT3;1* is required for maintenance of AMF symbiosis, the degree of AMF colonization and AMF morphology were compared in maize roots of *ZmAMT3;1-RNAi* lines (*3–18* and *3–46*) with the corresponding WT after 28, 35, and 42 dpi (Figure 6, D–F; Supplemental Figure S10, A–D). The total root colonization levels reached up to 80% and did not differ between WT and RNAi lines. Among these genotypes, the percentage of the root length in which hyphae, vesicles and arbuscules were found was also similar. These results indicate that the function of *ZmAMT3;1* was not crucial for AMF colonization and development in maize roots.

In a pot experiment, a $^{15}NH_4^+$-labeled soil patch allowing exclusive access to AMF hyphae, was placed for tracing N transfer from AMFs to host plants (Figure 7A). At 42 dpi, the roots of all genotypes were AMF-colonized as revealed by ∼60% root length colonization, and the mycorrhizal responses in shoot dry weight ranged from 30% to 50% (Supplemental Figure S11, A–D). Based on hyphal length density (HLD), we observed substantial hyphae in the ^{15}N-labeling pipes wrapped with a membrane of 30 μm pore size (30-μm Myc), but not in pipes wrapped with a membrane of 0.45 μm (0.45-μm Myc) (Supplemental Figure S11, E and F). For the AMF colonization and plant growth responsiveness, no genotypic differences were observed between WT and RNAi lines. However, the shoot ^{15}N abundance of WT plants that permitted AMF access to the ^{15}N-labeling pipes (30-μm Myc) was significantly greater than that of WT plants that were denied AMF access to labeling pipes (0.45-μm Myc) (Figure 7, B and C). As the hyphae reached the ^{15}N-labeling pipes by crossing the 30 μm membrane, the shoot ^{15}N increment can be assumed to be

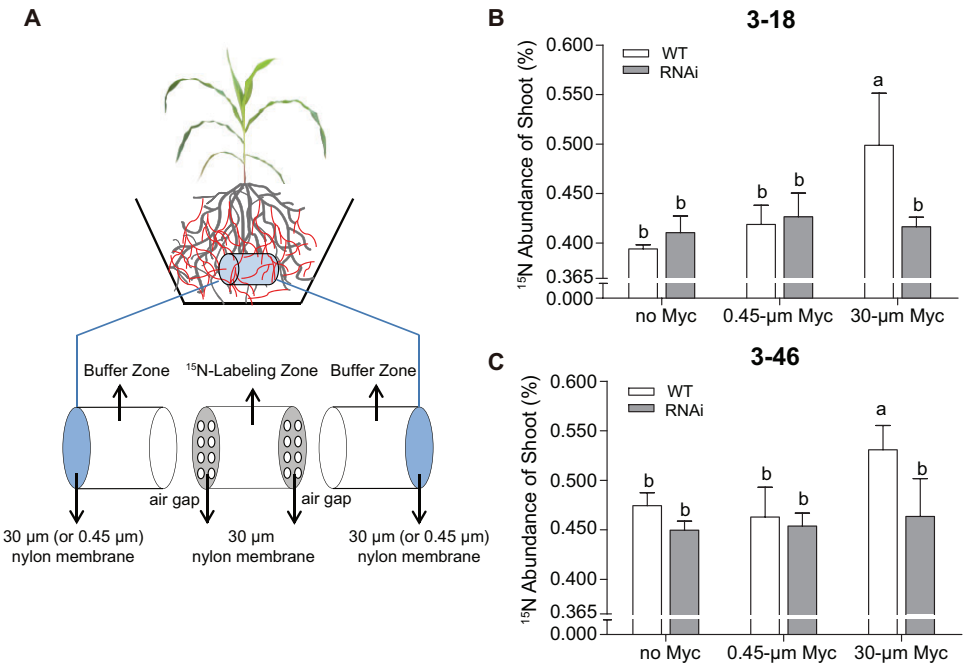

Figure 7 ZmAMT3;1 mediated ^{15}N transfer from AMF to maize plants. A, Illustration of device for ^{15}N-labeled soil patch in pot experiments. B and C, ^{15}N abundances of shoots in WT and two independent RNAi lines *3–18* (B) and *3–46* (C). "no Myc" indicates mock-inoculated control. "0.45-μm Myc" means that roots were colonized by AMF, and both roots and hyphae were prevented to enter the ^{15}N-labeling zone by a 0.45 μm membrane. "30-μm Myc" permitted access of hyphae but denied access of roots to ^{15}N-labeling zone by 30 μm membrane. For each treatment, data are means ± SD (n = 4, biological replicates). Different lowercase letters indicate significant differences by two-way ANOVA (Duncan's F-test, $P < 0.05$).

derived from $^{15}NH_4^+$ uptake via hyphae from the ^{15}N soil patch and subsequent transfer from AMFs to host plants. In both RNAi lines, however, this mycorrhiza-dependent shoot ^{15}N accumulation was completely lost, indicating a crucial role of ZmAMT3;1 in transferring N from AMFs to plants (Figure 7, B and C). These results were further supported by a second independent experiment (Supplemental Figure S12, A and B). Irrespective of WT or RNAi lines, the shoot ^{15}N accumulation did not differ between treatments of 0.45-μm Myc and no Myc, where no AMF hyphae could reach the ^{15}N-labeled soil patch (Figure 7, B and C; Supplemental Figure S12, A and B). Taken together, we conclude that ZmAMT3;1 was essential for Myc-N uptake in maize.

ZmAMT3;1 dominates the Myc-N pathway and substantially contributes to overall plant N nutrition

To quantify the physiological contribution of the ZmAMT3;1-dependent Myc-N uptake to the overall plant N acquisition, we established two types of pot experiments: the common compartment (roots and hyphae mixed; Supplemental Figure S13A) and separated compartment (roots and hyphae separated; Figure 8A). For WT in the common compartment experiment, compared with noninoculated plants, we observed significant increases of shoot dry weight in mycorrhizal plants at 42 dpi that revealed 30%–40% root length colonization (Supplemental Figure S13, B and C). Shoot N and P contents also increased in mycorrhizal plants along with induction of *ZmAMT3;1* and *ZmPht1.6* expression levels (Supplemental Figure S13, D–G). These traits, however, did not differ in both RNAi lines from those in the corresponding WT, except for the slightly lower shoot N contents in RNAi lines where most of the *ZmAMT3;1* transcripts were silenced (Supplemental Figure S13, B–G). Therefore, with mixed root-hyphae, we failed to find a relevant contribution of ZmAMT3;1-dependent Myc-N to overall N accumulation, which was then probably dominated by the Root-N uptake pathway.

In the separated compartment experiment, the hyphal compartment (HC) that was separated from the root compartment (RC) excluded the effect of Root-N uptake, allowing quantification of the contribution of Myc-N to overall plant N acquisition (Figure 8A). Compared with nonmycorrhizal plants, roots of WT and RNAi lines in RC were all substantially colonized by AMF at 42 dpi as revealed by $\sim 10^4$ increases of *Ri* gene copy numbers (Supplemental Figure S14, A and B). As expected, access of hyphae in HC was found in the 30-μm Myc treatment but not in the 0.45-μm Myc treatment (Supplemental Figure S14, C and D). In RC, there was a considerable proportion of hyphae, irrespective of 30-μm and 0.45-μm Myc treatments. No difference in root length colonization, total hyphal length, or in shoot biomass was observed between WT and RNAi plants (Supplemental Figure S14, A–F). For WT plants, the 30-μm Myc treatment allowed access of AMF hyphae to the HC for extra N capture, and subsequently the shoot N content increased by 9.6 ± 1.8 mg (corresponding WT for 3–18) and

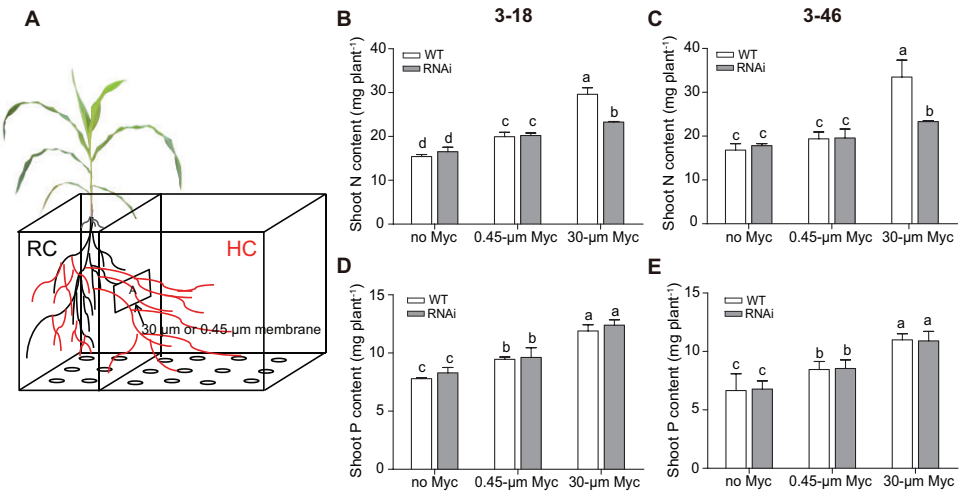

Figure 8 Quantitative ZmAMT3;1-mediated Myc-N uptake to overall plant N acquisition. A, Illustration of a microcosm device for a separated compartment pot experiment. B–E, Shoot N content (B and C), P content (D and E) in WT and RNAi lines (*3–18* and *3–46*) under different treatments. "no Myc" indicates mock-inoculated control. "0.45-µm Myc" means that root was colonized by AMF, and both roots and hyphae were prevented from entering the HC by a 0.45 µm membrane. "30-µm Myc" permitted access of hyphae but denied access of roots to the HC by a 30 µm membrane. For each treatment, data are means ± SD (n = 4, biological replicates). Different lowercase letters indicate significant differences by two-way ANOVA (Duncan's F-test, $P < 0.05$).

14.1 ± 4.2 mg (corresponding WT for 3–46) (Myc-N in HC = [30-µm Myc] − [0.45-µm Myc]) (Figure 8, B and C). These increments of shoot N content, representing Myc-N uptake by HC hyphae, accounted for 33% ± 5.8% and 42% ± 11.4% of overall shoot N accumulation. For two RNAi lines, however, the increased shoot N accumulation was substantially less, 3.1 ± 0.6 mg (lines 3–18) and 3.7 ± 2.0 mg (lines 3–46) due to silencing of *ZmAMT3;1* gene expression (Figure 8, B and C). This indicates that 68% ± 14.9% and 74% ± 24.5% of the capacity of Myc-N uptake from the HC was conferred by the ZmAMT3;1 protein. Although significant contributions of AMFs to N acquisition were also determined in the RC (Myc-N in RC = [0.45-µm Myc] − [no Myc]), they did not differ between WT and RNAi lines. Additional analysis of the shoot P contents revealed that in WT plants Myc-P uptake from the HC accounted for 21% ± 4.8% (3–18 event) and 23% ± 7.8% (3–46 event) of overall shoot P accumulation (Figure 8, D and E). However, we found no difference in Myc-P uptake between WT and RNAi plants (22% ± 7.7% in lines 3–18; 22% ± 9.9% in lines 3–46), indicating an exclusive function of ZmAMT3;1 in the Myc-N pathway.

The ZmAMT3;1-dependent Myc-N pathway contributes significantly to postsilking N uptake in field-grown maize

We subsequently assessed the contribution of the ZmAMT3;1-mediated Myc-N pathway to N uptake of field-grown maize at different developmental stages (jointing, silking, and maturation stages) during 2 years (2018 and 2019). During the main growth periods, shoot biomass and N content of maize plants gradually increased and reached a maximum at maturation (Figure 9, A–D; Supplemental Figure S15, A–D). At the jointing and silking stages, we found no significant differences in shoot N content between WT and RNAi lines. At maturation, however, RNAi lines *3–18* and *3–46* showed a significant reduction in shoot N accumulation, of 15.1%–17.7% and 12.9%–14.0%, respectively, compared with corresponding WT (Figure 9, A–D). The root length colonization by AMFs did not differ between WT (30.1% ± 2.5%) and RNAi line (30.4% ± 10.7%). For WT plants, the postsilking N uptake ranged between 776–800 mg (2018) and 925–1,275 mg (2019) N per plant, accounting for 40%–50% of overall N uptake during the whole growth period (Figure 9, A–D). However, the postsilking N uptake of the two RNAi lines was substantially reduced, by 252–275 mg (2018) and 507–740 mg (2019) N per plant. We, therefore, conclude that 33%–58% of postsilking N uptake was contributed by the ZmAMT3;1-mediated Myc-N pathway under field conditions.

Discussion

Improving N-acquisition efficiency (NAE) in crops is a great challenge for sustainable agriculture. Exploring the potential of interactions between plants and microorganisms to improve crop NAE is a promising approach (Fitter et al., 2011; Peiffer et al., 2013; Kuypers et al., 2018; Tao et al., 2019; Zhang et al., 2019a; Dellagi et al., 2020). Although AMF is the most widespread symbiotic relationship among plants, the benefits of AMF to plant N nutrition are still under debate, especially under field conditions (Smith et al., 2011; Smith and Smith, 2011; Wang et al., 2018; Makarov 2019). Our research demonstrated that the ZmAMT3;1 transporter mediated ammonium transport across the plant–AMF symbiotic interface and that this ZmAMT3;1-dependent Myc-N uptake contributed substantially to overall plant N acquisition under both laboratory and field conditions. These findings disentangle the molecular mechanisms and functions of AMF-associated N acquisition and highlight the quantitative

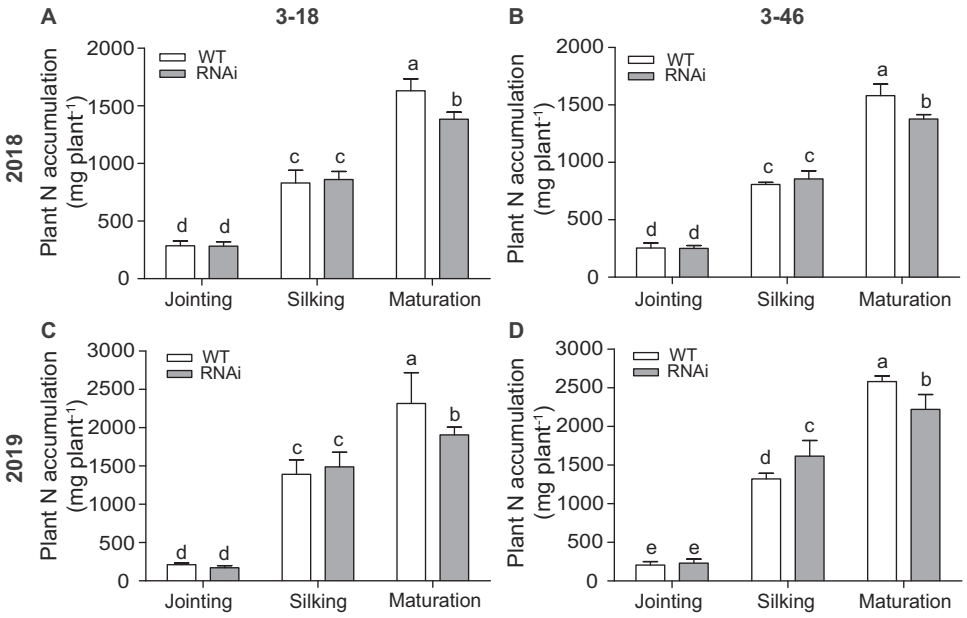

Figure 9 Contribution of the ZmAMT3;1-mediated Myc-N pathway to postsilking N uptake in field-grown maize. A–D, Plant N accumulation in shoots of WT and two independent transgenic lines (*3–18* and *3–46*) at different developmental stages across years of 2018 (A and B) and 2019 (C and D). Data are presented as means ± SD (n = 4, biological replicates). Different lowercase letters indicate significant differences by two-way ANOVA (Duncan's F-test, $P < 0.05$).

importance of this plant–microbe interaction for improving crop NAE.

ZmAMT3;1 mediates NH_3 transport across the symbiotic interface to deliver N from AMF to maize plants

AMF-inducible AMTs might be expected to play a role in Myc-N uptake, but direct molecular evidence for a contribution of these AMTs to plant N acquisition was still lacking (Smith and Smith, 2011; Bücking and Kafle, 2015; Makarov 2019; Dellagi et al., 2020). We provide three lines of evidence in maize that ZmAMT3;1 acts as a major component of this Myc-N pathway, conferring NH_3 transport across the PAM and mediating N delivery from AMF to the host plants.

First, like all AMF-inducible transporters, the *ZmAMT3;1* transcript and protein abundance were strongly upregulated by AMF inoculation (Figures 1 and Figure 5, A and B). The *ZmAMT3;1* transcript was exclusively expressed in arbuscule-containing cortical cells (Figure 2, A–G), and the encoded protein was targeted only to the PAM, and not to the plasma membrane of cortical cells (Figure 2G). Like the polar localization of MtPT4 and SbAMT3;1 (Pumplin et al., 2012; Koegel et al., 2013), the ZmAMT3;1 protein exclusively resided around arbuscule branches, indicating a role in nutrient or signal exchange between AMF and the host plants.

Second, the ZmAMT3;1 protein transported ammonium across the plasma membrane in yeast and oocytes (Figure 3, A and D). The relatively high affinity for ammonium (K_m = 16.6 μM, Figure 3B) of ZmAMT3;1 allows plants to compete with AMF for ammonium uptake in their interfacial space, where a high-affinity fungal AMT GintAMT2 resides in the internal hyphae (Pérez-Tienda et al., 2011). The pH-independence of ZmAMT3;1 activity may suggest the recruitment of NH_4^+ by the ZmAMT3;1 transporter (Figure 3A; Supplemental Figure S4). Indeed, as a common feature of all AMTs, the cation NH_4^+ is recruited to an external cation binding site. During transit through the narrowest region of the AMT pore, NH_4^+ is then deprotonated in a process involving His residues (Ariz et al., 2018; Ganz et al., 2020). Depending on the AMT type, the produced H^+ is either co-transported with NH_3 through the pore, or H^+ stays outside, with implications for the pH (Ariz et al., 2018; Brito et al., 2020; Ganz et al., 2020). A recent study demonstrated that EcAmtB in *Escherichia coli* transports ammonium as a NH_3/H^+ symporter that transports the neutral NH_3 and protons via two distinct pathways (Williamson et al., 2020). Plant AMT2-type AMTs belong to the same MEP-subfamily as EcAmtB (McDonald et al., 2012). However, the AMT2 members investigated so far including AMF-inducible ZmAMT3;1 and LjAMT2;2, are all electroneutral transporters of NH_3, although they apparently recognize NH_4^+ as the substrate (Figure 3, D–F; Guether et al., 2009; Neuhäuser et al., 2009; Straub et al., 2014). Given an acidic environment in the peri-arbuscular space, ionic NH_4^+ is expected to be the dominant species of ammonium (Guttenberger, 2000). With an electroneutral transport property, NH_4^+ must be deprotonated prior to its transport and uncharged NH_3 is then transported across the PAM into the plant symplast. It is assumed that this electroneutral transport may be driven by the NH_3 concentration gradient across the PAM, as AMF would release large amounts of ammonium in the symbiotic interface (Govindarajulu et al., 2005; Jin et al., 2005) while inoculated roots maintain a low cytosolic ammonium concentration by rapid assimilation of ammonium

(Wang et al., 2020). The fate of the released proton remains unsolved. Nevertheless, leaving protons in the interfacial space may help the symbionts to reduce energy costs for generating a H^+ electrochemical potential gradient via plant and fungal H^+-ATPases (Krajinski et al., 2014; Wang et al., 2014; Liu et al., 2020).

Third, the ^{15}N transfer from AMF to the host plant was completely lost in transgenic maize plants by RNAi silencing of *ZmAMT3;1* (Figure 7), showing the dominant role of ZmAMT3;1 in the Myc-N pathway under these conditions. Although the *ZmAMT4;1* gene also showed AMF-inducibility, its function in Myc-N uptake was likely negligible, owing to the extremely low transcript abundance (Figure 5A). Unlike the sensor function of MtAMT2;3 in regulating premature arbuscule degeneration in *M. truncatula* (Breuillin-Sessoms et al., 2015), in transgenic maize lines silencing of *ZmAMT3;1* did not affect the AMF symbiosis, in terms of AMF morphology and root colonization (Figure 6, D–F; Supplemental Figure S10) and the growth responsiveness to AMF was also not affected (Supplemental Figures S13 and S14). In these lines, with AMF, we observed a reduced plant N content, but neither a reduced plant P content nor Myc-specific *ZmPht1;6* expression levels (Figure 8, B–E; Supplemental Figure S13, D–G). This clearly indicates that N and P acquisition through the mycorrhizal pathways in maize are independent. In contrast, the knock-down mutations for the rice orthologue gene *OsAMT3;1* not only reduced symbiotic N uptake, but also symbiotic P uptake and abolished plant growth stimulation by AMF (Koegel et al., 2017). Considering that OsAMT3;1 was unable to transport ammonium (Supplemental Figure S3; Koegel et al., 2017), we surmise that OsAMT3;1, like MtAMT2;3, conveys a function in ammonium sensing, rather than ammonium transport. In contrast, ZmAMT3;1 directly mediated NH_3 transport from the interfacial apoplast into the plant symplast across the PAM, representing a key component of the Myc-N pathway in maize.

The ZmAMT3;1-dependent Myc-N pathway significantly contributes to overall plant N acquisition at later stages under field conditions

Previous attempts to quantify the physiological contribution of Myc-N uptake to overall plant N nutrition used different experimental systems and growing conditions (Corrêa et al., 2014; Nouri et al., 2014; Corrêa et al., 2015). However, it is difficult to draw solid conclusions due to lack of functionally characterized key component of the Myc-N pathway and the corresponding mutants. Additionally, the significance of the Myc-N pathway is hard to interpret, because of the difficulty of assessing whether improvement of plant N nutrition is conferred by direct N transfer from AM fungi or by indirect stimulatory effects from the AM symbiosis (Makarov, 2019). In this study, we discovered the function of ZmAMT3;1 exclusively in NH_3 transport at the symbiotic interface, not in plant-AMF symbiosis and symbiotic P uptake, thereby allowing quantification of the direct Myc-N transport using *ZmAMT3;1*-gene silenced plants. Using a separate compartment, accessible to the fungi only and not to the maize roots, where ammonium was supplied as N source, we showed that at least 30% of the shoot N accumulation was derived from the AMF symbiosis (Figure 8, B and C), in agreement with 20%–74% of overall plant N uptake in numerous previous studies using similar experimental systems (Tanaka and Yano, 2005; Corrêa et al., 2015; Thirkell et al., 2016). With this Myc-N uptake capacity, 68%–74% of N acquisition was conferred by ZmAMT3;1 (Figure 8, B and C). A much smaller proportion (~20%) of Myc-N uptake was found in *ZmAMT3;1*-RNAi lines which might be explained by residual ZmAMT3;1 activity. This may also be explained by a symbiotic nitrate uptake pathway, since a rice mutant defective in a Myc-specific nitrate transporter gene *OsNPF4.5* revealed a 45% decrease of symbiotic N uptake when NO_3^- was supplied as the N source (Wang et al., 2020). In analogy, its maize ortholog gene *ZmNPF4.5* might play a minor role in the Myc-N pathway. Indeed, expression levels of *ZmNPF4.5* were remarkably upregulated by AMF, as revealed by the transcriptome analysis (Supplemental Figure S1). Given that AMF prefer to take up soil ammonium over nitrate (Tanaka and Yano, 2005) and the N source in the symbiosis interface is mainly ammonium (Govindarajulu et al., 2005; Jin et al., 2005; Tian et al., 2010), AMT-mediated ammonium transport across the PAM is supposed to be the dominant pathway over NPF-mediated nitrate transport for Myc-dependent N acquisition.

A meta-analysis revealed that AMF inoculation, on average, increases grain yield by 16% under field conditions (Zhang et al., 2019b). Improved N acquisition by AMFs is often considered one of the main factors accounting for this yield increase (Cavagnaro et al., 2006; Zhang et al., 2015). However, some studies found no beneficial or even negative effects on yield by AMFs (Miller et al., 2002; van der Heijden et al., 2006; Ryan and Graham, 2018; Wang et al., 2018). Here, we show a significant contribution of Myc-N at the postsilking stage of field-grown maize. During the reproductive stage, the sink strength of developing grain increases, whilst root activity and growth decline, which may reduce the Root-N uptake capacity. The Myc-N pathway is then presumably relevant due to a significant AMF colonization during this period (Schalamuk et al., 2004; Buade et al., 2020). In later stages, ammonium may become the dominant N form in soil due to active organic N mineralization and nitrate leaching (Yao et al., 2021). Advantages of Myc-N then arise as AMFs not only prefer ammonium over nitrate but can also accelerate decomposition and acquire N from organic material (Hodge et al., 2001; Tanaka and Yano, 2005 Hodge and Fitter, 2010). In line with the higher expression levels of *ZmAMT3;1* at later developmental stages of maize (Figure 1, E–H), an increased contribution of ZmAMT3;1-dependent Myc-N is expected later in development. Indeed, the field trials revealed that 33%–58% of postsilking N uptake, accounting for ~15% of total N uptake, was supported by the ZmAMT3;1-mediated Myc-N pathway (Figure 9). We,

therefore, provided evidence for substantial benefits of Myc-N to maize NAE in the field.

Plants may adjust their nutrient-acquisition strategies by increasing their AMF colonization (Wang et al., 2017). The trade-off between the direct root and the symbiotic pathways may be expected to increase overall nutrient absorption. For P nutrition, the Pi transporters for the root uptake pathway are downregulated in response to AMF colonization, and the Myc-P pathway then dominates the overall plant Pi uptake (Smith et al., 2003, 2004; Yang et al., 2012). Transcriptional regulation is an important primary means of controlling Root-P absorption (Liu et al. 1998; Paszkowski et al., 2002; Grunwald et al., 2009). Interestingly, with AMF inoculation, the expression of epidermis-expressed AMTs *ZmAMT1;1a* and *ZmAMT1;3* for the Root-N pathway were suppressed at the protein level, but not at the transcriptional level (Figure 5). Additionally, phosphorylation modifications occurred at the conserved C-terminal region of the ZmAMT1;1a and ZmAMT1;3 proteins, potentially inactivating transporters responsible for the Root-N uptake pathway. In colonized maize roots, the transcript and protein abundance of ZmAMT3;1 significantly increased, and the dephosphorylated status of its CTR domain was in favor of an active contribution to the Myc-N uptake (Figures 4, B and C and 5; Supplemental Figure S7). Our results revealed a regulatory mechanism for the trade-off between Root-N and Myc-N pathways via the multi-level regulation of *ZmAMTs*.

Taken together, our results indicate that the Myc-N pathway is crucial for N acquisition of maize, especially for post-silking N uptake in the field. Therefore, we propose the following model for a Myc-N -uptake pathway in maize roots (Figure 10). Under AMF inoculation, ERM absorb N in the form of inorganic or organic N and metabolize it into Arg, which is translocated into IRM together with Poly-P. In the IRM, these transport forms are catabolized and NH_4^+ (or NH_3) is released from the IRM to the interfacial apoplast. The NH_4^+ is transferred to the root cells by the ZmAMT3;1 transporter likely in the form of NH_3. The parallel existence of both uptake systems might lead to undesirable trade-offs, because the Root-N uptake activity declines with increasing root AMF colonization. This may underestimate the contribution of ZmAMT3;1-dependent Myc-N uptake to overall plant N nutrition. Identification of upstream regulators modulating Root-N and Myc-N pathways will be of great interest for further research.

Methods

RNA extraction and transcriptomic analysis by Illumina sequencing

Total RNA was extracted from plant samples using RNAiso Plus Kit (TaKaRa, Kusatsu, Japan) according to the manufacturer's instructions. Library construction was performed using the NEB Next Ultra RNA Library Prep Kit for Illumina (New England Biolabs, Ipswich, MA, USA) with NEB Next Multiplex Oligos for Illumina (New England Biolabs) and were then sequenced using an Illumina HiSeq X Ten System. The sequence reads were mapped to the maize (*Z. mays*) B73 reference genome V3 using the Tophat2 software (Kim et al., 2013). Fragments per kilobase of transcript length per million mapped reads were used to estimate levels of gene expression by the Cufflinks software (Trapnell et al., 2010). All raw sequence reads from each sample are available on the NCBI with the BioProject ID: PRJNA833589.

Membrane protein isolation and phosphor-proteomics analysis

A microsomal fraction (MF) was extracted according to Wu et al. (2017). A total of 4 g of frozen roots was homogenized in 20 mL extraction buffer (330 mM sucrose, 100 mM KCl, 1 mM EDTA, 50 mM Tris-MES, fresh 5 mM dithiothreitol, and 1 mM phenylmethylsulfonyl fluoride, pH 7.5) in the presence of 0.5% v/v proteinase inhibitor mixture (Sigma-Aldrich, St. Louis, MO, USA) and phosphatase inhibitors (25 mM NaF, 1 mM Na_3VO_4, 1 mM benzamidin, 3 μM leupeptin). The microsomal pellet was re-suspended in 200 μL UTU (6 M urea, 2 M thiourea, pH 8). Protein concentration was determined using the Bradford assay (Sigma-Aldrich, St. Louis, MO, USA) with BSA as a standard. About 200 μg MF from roots was digested with sequencing-grade modified trypsin (Promega, Madison, WI, USA), and phosphopeptides were enriched using titanium dioxide (TiO_2) (GL Sciences, Japan) and desalted over a C_{18}-Stage tips prior to mass spectrometric analysis. Protein identification and ion intensity quantitation were carried out by software MaxQuant (version 1.5.3.8; Cox and Mann, 2008). Proteomic and phosphorsite data visualization and statistical analyses were conducted as described by Wu et al. (2019b).

RT-qPCR

First-strand cDNA was generated using the PrimeScriptTM RT reagent Kit with gDNA Eraser (TaKaRa, Kusatsu, Japan). qPCR was performed using the SYBR Premix Ex Taq II (TaKaRa, Kusatsu, Japan). A 7500 Real-Time PCR System (ABI, USA) was used to carry out the three-step PCR procedure. A maize gene *ZmAlpha-tubulin 4* (*ZmTUB4*) was used as the internal control for normalizing gene expression. Relative expression levels were calculated using a mathematical model established by Pfaffl (2001).

Gene cloning and plasmid constructs

The open reading frame of *ZmAMT3;1* (*ZmAMT3;1-ORF*) was amplified and cloned into vector pGEM-T-Easy vector (Promega, Madison, WI, USA). Mutations, as listed in Supplemental Table S2, were introduced into *ZmAMT3;1-ORF* sequences by using the Q5 Site-Directed Mutagenesis Kit (New England Biolabs, Ipswich, MA, USA). The fragments of *ZmAMT3;1-ORF* variants were then sub-cloned into the oocyte expression vector *pOO2* and the yeast expression vector *pDR196* through the restriction sites *Spe* I and *EcoR* I. For subcellular localization analysis, a chimeric DNA fragment encoding ZmAMT3;1 C-terminal fused GFP protein was inserted into the vectors under the control of the *CaMV 35S* promoter, yielding constructs of *p35S::ZmAMT3;1-GFP-pBI121* and

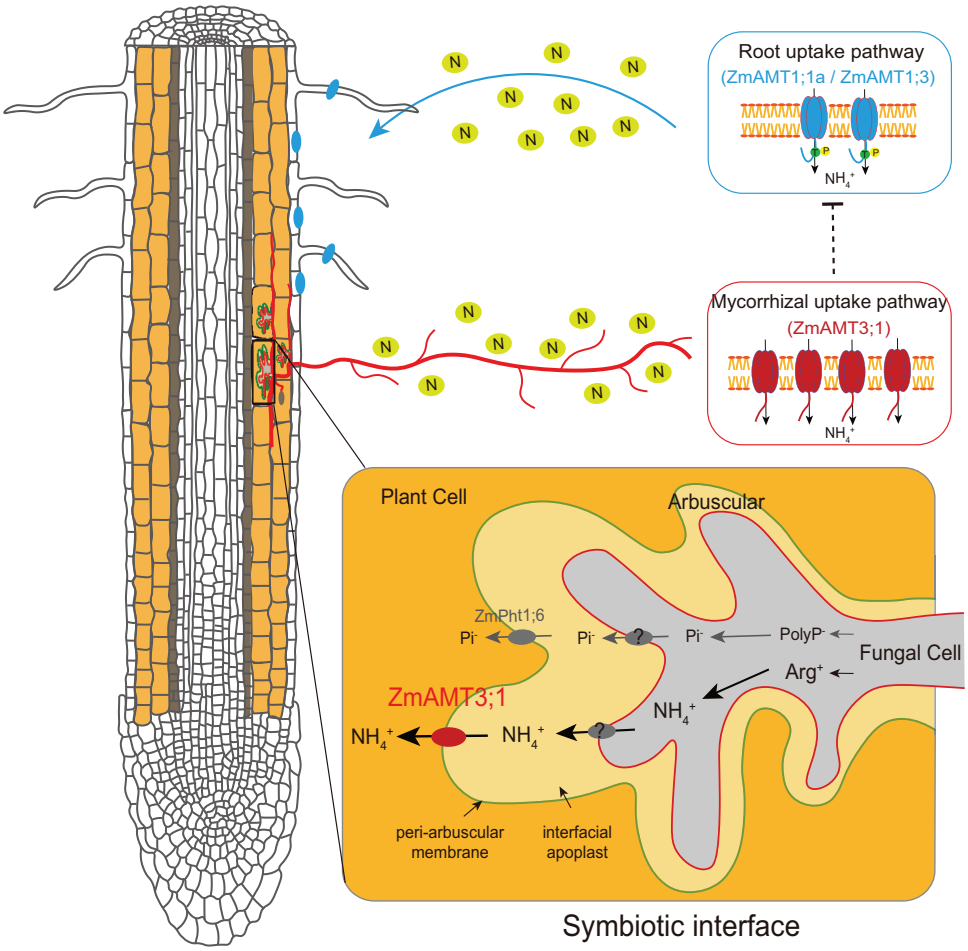

Figure 10 A model illustrating the arbuscular mycorrhiza-dependent ammonium uptake pathway in maize roots. Symbiotic plants exhibit two N-uptake pathways, direct root uptake (Root-N pathway) and mycorrhizal uptake (Myc-N pathway). For the Myc-N pathway, the ERM absorbs N and rapidly metabolizes it into Arg, which is translocated to the IRM together with PolyP compounds. After Arg is catabolized in the IRM, and ammonium is produced, this is released into the interfacial apoplast by an unknown mechanism (Tian et al., 2010). The NH_4^+ ion is then recruited by the PAM-localized AMT ZmAMT3;1, becomes deprotonated, and uncharged NH_3 is likely transported into root cells. For the Myc-P pathway, phosphate is released by unknown transporters into the apoplast, and then transported into root cells by a PAM-localized H^+/Pi symporter ZmPht1;6 (Willmann et al., 2013). In mycorrhizal roots, ZmAMT3;1 transcripts and proteins are upregulated, thus inducing the Myc-N pathway, while the protein abundance and activity of the epidermis-expressed ZmAMT1;1a/ZmAMT1;3 responsible for Root-N pathway are suppressed. Under greenhouse and field conditions, the ZmAMT3;1-mediated Myc-N pathway contributes significantly to plant overall N acquisition.

p35S::ZmAMT3;1-GFP-pEZS-NL for transient expression in epidermal cells and maize protoplast cells, respectively. The ZmAMT3;1 C-terminal fused GFP protein was also subcloned into the *pOO2* vector through the restriction sites *Spe* I and *Xba* I, used for localization of ZmAMT3;1 in oocytes.

To generate the *pUbi::ZmAMT3;1-RNAi* construct, a fragment of 411 bp *ZmAMT3;1-ORF* (916–1,327 bp) was introduced by *BamH* I/*Kpn* I and *Sac* I/*Spe* I for the sense and antisense sequence, respectively, into an RNAi vector pTCK303 under the control of maize *Ubiquitin 1* gene promoter (Wang et al., 2004). For promoter-GUS and promoter-gene-GFP analysis, the promoter of the *ZmAMT3;1* gene was amplified (~3.0 kb) and sub-cloned into the pCAMBIA3,301 vector by *Hind* III and *Nco* I, yielding the *pZmAMT3;1pro::GUS* construct. The fragment of *ZmAMT3;1-GFP* was introduced into the p1,301-Ubi-PPT vector under control of the *ZmAMT3;1* promoter by *Sac* I and *Hind* III, yielding the *pZmAMT3;1pro::ZmAMT3;1-GFP* construct. All primers used in this study are listed in Supplemental Table S1.

Maize transformation and transient expression in maize protoplasts

The *pUbi::ZmAMT3;1-RNAi*, *pZmAMT3;1pro::GUS*, and *pZmAMT3;1pro:: ZmAMT3;1-GFP* plasmids were transformed into the *Agrobacterium tumefaciens* strain EHA105 using the freeze-thaw method. A single colony was selected to transform immature embryos of maize hybrid Hi-II (HA × HB) using the method of An et al. (2014). The T3 homozygous lines were selected for GUS staining and GFP analysis. Regarding the RNAi lines, the regenerated plantlets were backcrossed with inbred line B73, and the BC_3F_2 homozygote lines were selected for pot and field experiments.

The *p35S::ZmAMT3;1-GFP-pEZS-NL* construct was transformed into maize mesophyll protoplasts by polyethylene glycol mediated transformation as described by Yoo et al. (2007). The mixture of protoplasts and plasmids was cultured overnight, and the green fluorescence signals derived from GFP and the red fluorescence signals from the membrane-specific dye FM4–64 (Sigma-Aldrich, St. Louis, MO, USA) were examined using a confocal laser scanning microscope (LSM 880, Carl Zeiss, Germany).

In situ RNA hybridization, GUS histochemical staining, and confocal GFP fluorescence scanning

In a greenhouse, maize plants were grown in soil in pots inoculated with *Ri* fungus and sampled at 42 dpi. In situ RNA hybridization was performed as previously described (Gu et al., 2013). The root segments from inoculated maize (var B73) were harvested and fixed in FAA (50% ethanol, 5% acetic acid, and 10% formalin containing 37% formaldehyde) for 12 h at 4°C. Paraffin-embedded root section with 8–12 μm thickness were generated. Digoxigenin (DIG)-labeled RNA sense and antisense probes were synthesized by in vitro transcription using primers with the *T7* promoter sequence at the 5′ end and gene-specific linearized cDNA as templates, according to the DIG RNA Labeling Kit (Roche, Basel, Switzerland). The hybridization reaction was conducted at 50°C for 16 h. Anti-DIG alkaline phosphatase-conjugated antibody (Roche, Basel, Switzerland) and the NBT (nitro-blue tetrazolium)/5-bromo-4-chloro-3-indolyl phosphate (Roche, Basel, Switzerland) straining method were used. Photographs were observed by light microscopy (DP25 Olympus, Japan).

For analysis of *promoter-GUS* and *promoter-gene-GFP* reporter lines, the root segments from mycorrhizal inoculated transgenic maize plants *pZmAMT3;1pro::GUS* and *pZmAMT3;1pro::ZmAMT3;1-GFP* were harvested. For GUS staining, the samples were immersed in the GUS Histochemical Kit (RTU4032, Real-Times, China), placed under vacuum for 10 min and incubated at 37°C for 3 h. After decolorization in 70% ethanol overnight at RT, the maize roots were stained with WGA-Alexa Fluor 488 (Thermo Fisher Scientific, Waltham, MA, USA) and the GUS signals were then examined by fluorescence microscope (Eclipse Ti2, Nikon, Japan). The GFP fluorescence signals were examined using a confocal laser scanning microscope (LSM 880, Carl Zeiss, Germany).

Functional assays in yeast

The plasmids were transformed in triple-Δ*mep* (*1–3*) deletion yeast strain *31,019b* (Marini et al., 1997) by electroporation (MicroPulser, Bio-Rad, Hercules, CA, USA), and the transformants were selected on solid YNB medium with Arg (2%, w/v, Agar, YNB without amino acids and ammonium sulfate (Difco, BD, USA), 3%, w/v, glucose, and 0.1%, w/v, Arg). A growth complementation assay was performed on solid YNB medium supplemented with 3%, w/v, glucose and indicated N source, buffered with 50 mM MES/Tris (pH 5.5) at different pH. The ^{15}N-labeled ammonium uptake assay was performed at a desired concentration range from 10 to 500 μM of $^{15}NH_4^+$ (99.16 atom% ^{15}N, Shanghai Research Institute of Chemical Industry, China) as described by Loqué et al. (2009). The abundance of ^{15}N was identified by isotope ratio mass spectrometry (DELTAplus XP, Thermo-Finnigan, USA).

Functional assays in *Xenopus* oocytes

The electrophysiological assay was performed using methods as described by Mayer and Ludewig (2006). Oocytes were obtained from Ecocyte Bioscience (Castrop-Rauxel, Germany), presorted again and injected with 50 nL of cRNA (0.4 μg μL^{-1}). Oocytes were kept in ND96 for 4 days at 18°C and then placed in a small recording chamber. The recording solution was 110 mM choline chloride, 2 mM $CaCl_2$, 2 mM $MgCl_2$, and 5 mM MES, pH adjusted to 5.5 with Tris. Ammonium (3 mM) was added as NH_4Cl. The membrane potential of the oocytes was clamped to a resting potential of 0 mV. To measure NH_4^+-dependent currents, the potential was changed stepwise, starting at 40 mV, decreasing in steps of 20 mV down to −120 mV. The pulses were given for 50 ms with eight repetitions per trail. At each voltage, currents without added ammonium were then subtracted from currents with ammonium. For determination of ammonium uptake, oocytes were incubated for 30 min in recording solution additionally containing 3 mM ^{15}N ammonium from ammonium sulfate (98 a,tom% ^{15}N). Oocytes were washed 6 times in water, and separately transferred to tin cups for ^{15}N determination. In the pH-dependent uptake assay, the oocytes were incubated for three days after injections, to avoid damage by low pH. Uptake was performed in ND96 with pH adjusted to 4.5, 5.5, 6.5, and 7.5 containing 3 mM ^{15}N ammonium for 60 min. The fluorescence signals were examined in oocytes that were injected with the GFP fusion construct after 4 days using a confocal laser scanning microscope (LSM 880, Carl Zeiss, Germany).

Pot experiments in greenhouse

A calcareous loamy soil was collected from field plots at the China Agricultural University (CAU) Long-Term Fertilizer Station (Changping, Beijing, China). The soil was passed through a 2-mm sieve and sterilized by radiation with ^{60}Co γ-radiation at 10 kGy. Soil was then placed in plastic pots (Supplemental Figure S13A; 18 cm in height, 16 cm in diameter, and 2 kg of soil per pot). The basic nutritional composition of experimental soils is summarized in Supplemental Table S3; an additional 100 mg kg^{-1} NH_4^+-N, 20 mg kg^{-1} P, 200 mg K, 100 mg Mg, 5.5 mg Fe, 5 mg Cu, 5 mg Mn, and 5 mg Zn were added. Maize seeds of similar size were germinated in a sterile incubator for three days at 28°C, and the pregerminated seedlings were transplanted into pots containing soil. A total of 50 g (∼1,000 spores per plant) of *Ri* inoculum was added and mixed with the soils, and autoclaved inoculum was added as control (no mycorrhizal plants). To correct the possible differences in microbial communities, each pot received 10 mL of filtered AM fungal inoculum. Plants were grown in a greenhouse at day: night

temperatures of 28: 22°C and weekly re-randomized. We added a calculated amount of water to maintain the soil moisture at ~10%.

In the same pot experiment as above, a patch of ^{15}N-labeled soil was included to trace N transfer from AMF to host plants (Figure 7A). This microcosm consisted of three PVC pipes 2 cm in diameter and 2 cm in length. In the middle, a PVC pipe was set as ^{15}N-labeling zone, which contained 20 g soil with 2.6 mg ammonium sulfate-^{15}N (95Atom% ^{15}N). The two PVC pipes were used as buffer zones at both ends. The labeling zone was covered with a 30-μm nylon membrane to slow down solute diffusion from the labeling zone. A 30-μm nylon membrane was wrapped on both sides of the buffer zones which permitted access of AMF hyphae but prevented access of roots to the labeled zone. As a control, a 0.45-μm nylon membrane was wrapped to prevent access of both roots and AMF hyphae.

The separated compartments in the pot experiment were used as described by Thirkell et al. (2016) with a minor modification (Figure 8A). The compartment was split into an RC with size of 7 × 14 × 16 cm and a HC with size of 14 × 14 × 16 cm. A window cut in the abutting sides of the boxes created an aperture (4 × 6 cm). A double-ply 30-μm nylon membrane was used to cover the aperture, allowing exclusive access of AM hyphae from RC into HC. As a control, the 0.45 μm nylon membrane was then used to prevent access of hyphae into HC. About 1 kg Turface MVP (Profile Products LLC) as growth substrate was filled into RC and 2 kg Turface MVP into HC. Pregerminated maize seedlings were transplanted into RCs and a total of 50 mL (~1,000 spores per plant) of *Ri* inoculum was added and mixed with the substrate. Plants were grown in a growth cabinet in a 14 h/28°C and 10 h/22°C day-night rhythm, at a light intensity of 300 μmol m^{-2} s^{-1} and 70% humidity. Every week, each RC and HC received 50 and 100 mL, respectively, of nutrient solution (1 mM K_2SO_4; 0.6 mM $MgSO_4$; 35 μM KH_2PO_4; 0.5 mM $CaCl_2$; 0.1 M Fe-EDTA; 0.5 μM $ZnSO_4$; 0.5 μM $MnSO_4$, 1 μM H_3BO_3; 0.2 μM $CuSO_4$; 0.07 μM Na_2MoO_4; 2 mM NH_4NO_3 for RC, and 2 mM $(NH_4)_2SO_4$ for HC; pH 5.8–6.0). A total of 25.2 mg N and 0.56 mg P were added to the RC, and 137.2 mg N and 2.86 mg P were added to the HC.

Six-week-old plants were harvested, and fresh roots were collected. One subsample was subsequently frozen in liquid nitrogen for molecular analyses, and another subsample was used to determine AM colonization. Shoots were dried at 80°C for 72 h and weighed. N and P were measured using an elemental analyzer (vario Macro CNS, Elementar, Germany) and an Inductively coupled plasma mass spectrometry (ICP-OES, PerkinElmer, Waltham, MA, USA), respectively. The contribution of the Myc-N pathway to overall plant N uptake was calculated based on the difference of shoot N content of plants between 30-μm and 0.45-μm Myc treatments. The contribution of ZmAMT3;1-dependent activity to Myc-N uptake was then calculated based on the difference between the obtained Myc-N capacity of WT and RNAi plants.

Field trials

Field trials were carried out at the CAU experimental station in Shangzhuang, Beijing, China (40°06′N, 116°11′E, 46 m above sea level) in 2018 and 2019. The chemical properties of the 0–30 cm soil before sowing and fertilizer treatments are summarized in Supplemental Table S3. The fields were supplied with 75 kg ha^{-1} P, 135 kg ha^{-1} K, and 112 kg ha^{-1} N fertilizer, representing a moderately low N supply. The maize plants were evaluated in a completely randomized block design of one-row plots with four replications. Each row contained 17 plants with 50 cm inter-row spacing and 33 cm intra-row spacing. Standard cultivation management practices were used. Shoots of plants were harvested at jointing, silking, or maturation stage. N concentration was measured using a modified Kjeldahl acid-digestion method (Nelson and Sommers, 1973).

Mycorrhizal colonization and HLD analysis

Mycorrhizal colonization was assessed by the method of Trouvelot et al. (1986). Roots were cut into 1-cm segments and thoroughly mixed. A 0.5 g subsample was washed with 10% (*w*/*v*) KOH at 90°C for about 30 min, 2% H_2O_2 for 5 min at room temperature, and stained with trypan blue for 30 min at 90°C. For the pot experiment with separated compartments, mycorrhizal colonization was determined according to abundance of the *Ri* gene as described by Jansa et al. (2003). About 100 mg fresh roots were weighed for DNA extraction, and the copy number of the *Ri* gene was identified by qPCR using *Ri* strain-specific primers intra-1/-2. The HLD (meters of hyphae per gram of substrate) was determined according to Jakobsen et al. (1992). The soil or Turface MVP substrate in each pot was mixed, and subsamples were taken for determination of HLD.

Statistical analyses

The software SPSS version 18.0 (IBM, Chicago, IL, USA) was used for statistical analyses. Comparisons of sample means were made either by Student's t test ($P < 0.05$) or one-way or two-way analysis of variance ($P < 0.05$) followed by Duncan's post-hoc multiple comparisons tests, as shown in legends of Tables and Figures. The results are shown in Supplemental Data Set 1.

Accession numbers

Sequence data from this article can be found in the GenBank/EBML libraries under the following accession numbers: ZmAMT1;1a, GRMZM2G175140; ZmAMT1;1b, GRMZM2G118950; ZmAMT1;3, GRMZM2G028736; ZmAMT2;1, GRMZM2G080045; ZmAMT3;1, GRMZM2G335218; ZmAMT3;2, GRMZM2G338809; ZmAMT3;3, GRMZM2G043193; ZmAMT4;1, GRMZM2G473697; ZmPht1;6, GRMZM5G881088; OsAMT3;1, Os01g65000. The raw RNAseq data are deposited under BioProject PRJNA833589.

Supplemental data

The following materials are available in the online version of this article.

Supplemental Figure S1. Heatmap analysis of nitrate transporter genes *ZmNPFs* and *ZmNRT2s* expression by an RNA-seq approach.

Supplemental Figure S2. Plasma-membrane localization of the ZmAMT3;1-GFP fusion protein.

Supplemental Figure S3. Functional complementation of OsAMT3;1 in ammonium uptake-defective yeast strain *31019b* (ΔΔΔ*mep1;2;3*).

Supplemental Figure S4. ZmAMT3;1 protein activity in oocytes was independent of external pH.

Supplemental Figure S5. Ammonium transport activity of ZmAMT3;1 regulated by phosphorylation of the CTR.

Supplemental Figure S6. Measurement of ammonium-dependent inward current in the *Xenopus* oocytes expressing ZmAMT3;1 and the C-terminus phospho-mutants.

Supplemental Figure S7. Best representative annotated spectra identifying the phosphorylation site of ZmAMTs.

Supplemental Figure S8. Expression of *ZmAMTs* in *ZmAMT3;1*-RNAi transgenic maize lines.

Supplemental Figure S9. Expression of *ZmNPF4.5* and *ZmPht1;6* in *ZmAMT3;1*-RNAi transgenic maize lines.

Supplemental Figure S10. Silencing *ZmAMT3;1* gene did not affect mycorrhizal symbiosis.

Supplemental Figure S11. ZmAMT3;1 mediated ^{15}N transfer from AMF to maize plants.

Supplemental Figure S12. Independent second experiment on ZmAMT3;1-mediated ^{15}N transfer from AMF to maize plants.

Supplemental Figure S13. Quantification of ZmAMT3;1-mediated Myc-N uptake to overall plant N nutrition using the common compartment pot experiment.

Supplemental Figure S14. Quantification of ZmAMT3;1-mediated Myc-N pathway to overall plant N acquisition using the separated compartment pot experiment.

Supplemental Figure S15. Contribution of the ZmAMT3;1-mediated Myc-N pathway to postsilking biomass in field-grown maize.

Supplemental Table S1. List of primers used in this study.

Supplemental Table S2. Phospho-mutant variants for ZmAMT3;1 protein.

Supplemental Table S3. Physical-chemical properties of soils.

Supplemental Data Set 1. Results of statistical analyses.

Funding

This work was financially supported by the National Key Research and Development Program of China (grant no. 2021YFF1000500), the Natural Science Foundation of China (grant no. 31471934), and the Deutsche Forschungsgemeinschaft (DFG; 328017493/GRK 2366).

Conflict of interest statement. None declared.

References

Ariz I, Boeckstaens M, Gouveia C, Martins AP, Sanz-Luque E, Fernandez E, Soveral G, von Wiren N, Marini AM, Aparicio-Tejo PM, et al (2018) Nitrogen isotope signature evidences ammonium deprotonation as a common transport mechanism for the AMT-Mep-Rh protein superfamily. Sci Adv **4**: eaar3599

Bago B, Pfeffer P, Shachar-Hill Y (2001) Could the urea cycle be translocating nitrogen in the arbuscular mycorrhizal symbiosis? New Phytologist **149**: 4–8

Balestrini R, Brunetti C, Chitrra W, Nerva L (2020) Photosynthetic traits and nitrogen uptake in crops: which is the role of arbuscular mycorrhizal fungi? Plants **9**: 1105

Bravo A, Brands M, Wewer V, Dormann P, Harrison MJ (2017) Arbuscular mycorrhiza-specific enzymes FatM and RAM2 fine-tune lipid biosynthesis to promote development of arbuscular mycorrhiza. New Phytol **214**: 1631–1645

Breuillin-Sessoms F, Floss DS, Gomez SK, Pumplin N, Ding Y, Levesque-Tremblay V, Noar RD, Daniels DA, Bravo A, Eaglesham JB, et al (2015) Suppression of arbuscule degeneration in *Medicago truncatula phosphate transporter4* mutants is dependent on the ammonium transporter 2 family protein AMT2;3. Plant Cell **27**: 1352–1366

Brito AS, Neuhäuser B, Wintjens R, Marini AM, Boeckstaens M (2020) Yeast filamentation signaling is connected to a specific substrate translocation mechanism of the Mep2 transceptor. PLoS Genet **16**: e1008634

Buade R, Chourasiya D, Prakash A, Sharma MP (2020) Changes in arbuscular mycorrhizal fungal community structure in soybean rhizosphere soil assessed at different growth stages of soybean. Agric Res **10**: 32–43

Bücking H, Kafle A (2015) Role of arbuscular mycorrhizal fungi in the nitrogen uptake of plants: current knowledge and research gaps. Agronomy **5**: 587–612

Cavagnaro TR, Jackson LE, Six J, Ferris H, Goyal S, Asami D, Scow KM (2006) Arbuscular mycorrhizas, microbial communities, nutrient availability, and soil aggregates in organic tomato production. Plant Soil **282**: 209–225

Chalot M, Blaudez D, Brun A (2006) Ammonia: a candidate for nitrogen transfer at the mycorrhizal interface. Trends Plant Sci **11**: 263–266

Chen A, Gu M, Wang S, Chen J, Xu G (2018) Transport properties and regulatory roles of nitrogen in arbuscular mycorrhizal symbiosis. Semin Cell Dev Biol **74**: 80–88

Corrêa A, Cruz C, Ferrol N (2015) Nitrogen and carbon/nitrogen dynamics in arbuscular mycorrhiza: the great unknown. Mycorrhiza **25**: 499–515

Corrêa A, Cruz C, Pérez-Tienda J, Ferrol N (2014) Shedding light onto nutrient responses of arbuscular mycorrhizal plants: nutrient interactions may lead to unpredicted outcomes of the symbiosis. Plant Sci **221–222**: 29–41

Courty PE, Smith P, Koegel S, Redecker D, Wipf D (2015) Inorganic nitrogen uptake and transport in beneficial plant root-microbe interactions. Crit Rev Plant Sci **34**: 4–16

Cox J, Mann M (2008) MaxQuant enables high peptide identification rates, individualized p.p.b.-range mass accuracies and proteome-wide protein quantification. Nature Biotechnol **26**: 1367–1372

Dellagi A, Quillere I, Hirel B (2020) Beneficial soil-borne bacteria and fungi: a promising way to improve plant nitrogen acquisition. J Exp Bot **71**: 4469–4479

Fellbaum CR, Gachomo EW, Beesetty Y, Choudhari S, Strahan GD, Pfeffer PE, Kiers ET, Bücking H (2012) Carbon availability triggers fungal nitrogen uptake and transport in arbuscular mycorrhizal symbiosis. Proc Natl Acad Sci USA **109**: 2666–2671

Fitter AH, Helgason T, Hodge A (2011) Nutritional exchanges in the arbuscular mycorrhizal symbiosis: implications for sustainable agriculture. Fungal Biol Rev **25**: 68–72

Ganz P, Ijato T, Porras-Murrilo R, Stuhrwohldt N, Ludewig U, Neuhäuser B (2020) A twin histidine motif is the core structure

for high-affinity substrate selection in plant ammonium transporters. J Biol Chem **295**: 3362–3370

Glassop D, Smith SE, Smith FW (2005) Cereal phosphate transporters associated with the mycorrhizal pathway of phosphate uptake into roots. Planta **222**: 688–698

Govindarajulu M, Pfeffer PE, Jin H, Abubaker J, Douds DD, Allen JW, Bücking H, Lammers PJ, Shachar-Hill Y (2005) Nitrogen transfer in the arbuscular mycorrhizal symbiosis. Nature **435**: 819–823

Grace EJ, Cotsaftis O, Tester M, Smith FA, Smith SE (2009) Arbuscular mycorrhizal inhibition of growth in barley cannot be attributed to extent of colonization, fungal phosphorus uptake or effects on expression of plant phosphate transporter genes. New Phytol **181**: 938–949

Grunwald U, Guo W, Fischer K, Isayenkov S, Ludwig-Müller J, Hause B, Yan X, Kuster H, Franken P (2009) Overlapping expression patterns and differential transcript levels of phosphate transporter genes in arbuscular mycorrhizal, Pi-fertilised and phytohormone-treated *Medicago truncatula* roots. Planta **229**: 1023–1034

Gu R, Duan F, An X, Zhang F, von Wirén N, Yuan L (2013) Characterization of AMT-mediated high-affinity ammonium uptake in roots of maize (*Zea mays* L.). Plant Cell Physiol **54**: 1515–1524

Guether M, Neuhäuser B, Balestrini R, Dynowski M, Ludewig U, Bonfante P (2009) A mycorrhizal-specific ammonium transporter from *Lotus japonicus* acquires nitrogen released by arbuscular mycorrhizal fungi. Plant Physiol **150**: 73–83

Guttenberger M (2000) Arbuscules of vesicular-arbuscular mycorrhizal fungi inhabit an acidic compartment within plant roots. Planta **211**: 299–304

Hamel C, Smith DL (1991) Interspecific N-transfer and plant development in a mycorrhizal field-grown mixture. Soil Biol Biochem **23**: 661–665

Hao DL, Zhou JY, Yang SY, Huang YN, Su YH (2020) Functional and regulatory characterization of three AMTs in maize roots. Front Plant Sci **11**: 884

Hawkins HJ, George E (1999) Effect of plant nitrogen status on the contribution of arbuscular mycorrhizal hyphae to plant nitrogen uptake. Physiol Plant **105**: 694–700

Hawkins HJ, Johansen A, George E (2000) Uptake and transport of organic and inorganic nitrogen by arbuscular mycorrhizal fungi. Plant Soil **226**: 275–285

Hodge A, Campbell CD, Fitter AH (2001) An arbuscular mycorrhizal fungus accelerates decomposition and acquires nitrogen directly from organic material. Nature **413**: 297–299

Hodge A, Fitter AH (2010) Substantial nitrogen acquisition by arbuscular mycorrhizal fungi from organic material has implication for N cycling. Proc Natl Acad Sci USA **107**: 13754–13759

Jakobsen I, Abbott LK, Robson AD (1992) External hyphae of vesicular-arbuscular mycorrhizal fungi associated with *Trifolium subterraneum* L. New Phytol **124**: 61–68

Jansa J, Mozafar A, Kuhn G, Anken T, Ruh R, Sanders IR, Frossard E (2003) Soil tillage affects the community structure of mycorrhizal fungi in maize roots. Ecol Appl **13**: 1164–1176

Javot H, Penmetsa RV, Breuillin F, Bhattarai KK, Noar RD, Gomez SK, Zhang Q, Cook DR, Harrison MJ (2011) *Medicago truncatula mtpt4* mutants reveal a role for nitrogen in the regulation of arbuscule degeneration in arbuscular mycorrhizal symbiosis. Plant J **68**: 954–965

Jiang Y, Wang W, Xie Q, Liu N, Liu L, Wang D, Zhang X, Yang C, Chen X, Tang D, et al (2017) Plants transfer lipids to sustain colonization by mutualistic mycorrhizal and parasitic fungi. Science **356**: 1172–1175

Jin H, Pfeffer PE, Douds DD, Piotrowski E, Lammers PJ, Shachar-Hill Y (2005) The uptake, metabolism, transport and transfer of nitrogen in an arbuscular mycorrhizal symbiosis. New Phytol **168**: 687–696

Johansen A, Jakobsen I, Jensen ES (1993) Hyphal transport by a vesicular-arbuscular mycorrhizal fungus of N applied to the soil as ammonium or nitrate. Biol Fertil Soil **16**: 66–70

Keymer A, Pimprikar P, Wewer V, Huber C, Brands M, Bucerius SL, Delaux PM, Klingl V, Ropenack-Lahaye EV, Wang TL, et al (2017) Lipid transfer from plants to arbuscular mycorrhiza fungi. Elife **6**: 29107

Kim D, Pertea G, Trapnell C, Pimentel H, Kelley R, Salzberg SL (2013) TopHat2: accurate alignment of transcriptomes in the presence of insertions, deletions and gene fusions. Genome Biol **14**: R36

Kobae Y, Tamura Y, Takai S, Banba M, Hata S (2010) Localized expression of arbuscular mycorrhiza-inducible ammonium transporters in soybean. Plant Cell Physiol **51**: 1411–1415

Koegel S, Ait Lahmidi N, Arnould C, Chatagnier O, Walder F, Ineichen K, Boller T, Wipf D, Wiemken A, Courty PE (2013) The family of ammonium transporters (AMT) in *Sorghum bicolor*: two AMT members are induced locally, but not systemically in roots colonized by arbuscular mycorrhizal fungi. New Phytol **198**: 853–865

Koegel S, Mieulet D, Baday S, Chatagnier O, Lehmann MF, Wiemken A, Boller T, Wipf D, Berneche S, Guiderdoni E, et al (2017) Phylogenetic, structural, and functional characterization of AMT3;1, an ammonium transporter induced by mycorrhization among model grasses. Mycorrhiza **27**: 695–708

Krajinski F, Courty PE, Sieh D, Franken P, Zhang H, Bucher M, Gerlach N, Kryvoruchko I, Zoeller D, Udvardi M, et al (2014) The H+-ATPase HA1 of Medicago truncatula is essential for phosphate transport and plant growth during arbuscular mycorrhizal symbiosis. Plant Cell **26**: 1808–1817

Kuypers MMM, Marchant HK, Kartal B (2018) The microbial nitrogen-cycling network. Nat Rev Microbiol **16**: 263–276

Lanquar V, Loqué D, Hörmann F, Yuan L, Bohner A, Engelsberger WR, Lalonde S, Schulze WX, von Wirén N, Frommer WB (2009) Feedback inhibition of ammonium uptake by a phospho-dependent allosteric mechanism in *Arabidopsis*. Plant Cell **21**: 3610–3622

Leigh J, Hodge A, Fitter AH (2009) Arbuscular mycorrhizal fungi can transfer substantial amounts of nitrogen to their host plant from organic material. New Phytol **181**: 199–207

Liu H, Trieu AT, Blaylock LA, Harrison MJ (1998) Cloning and characterization of two phosphate transporters from *Medicago truncatula* roots: regulation in response to phosphate and to colonization by arbuscular mycorrhizal (AM) fungi. Mol. Plant Microbe Interact **11**: 14–22

Liu J, Chen J, Xie K, Tian Y, Yan A, Liu J, Huang Y, Wang S, Zhu Y, Chen A, et al (2020) A mycorrhiza-specific H^+-ATPase is essential for arbuscule development and symbiotic phosphate and nitrogen uptake. Plant Cell Environ **43**: 1069–1083

Loqué D, Lalonde S, Looger LL, von Wirén N, Frommer WB (2007) A cytosolic trans-activation domain essential for ammonium uptake. Nature **446**: 195–198

Loqué D, Mora SI, Andrade SL, Pantoja O, Frommer WB (2009) Pore mutations in ammonium transporter AMT1 with increased electrogenic ammonium transport activity. J Biol Chem **284**: 24988–24995

Ludewig U (2006) Ion transport versus gas conduction: function of AMT/Rh-type proteins. Transfus Clin Biol **13**: 111–116

Luginbuehl LH, Menard GN, Kurup S, Van Erp H, Radhakrishnan GV, Breakspear A, Oldroyd GED, Eastmond PJ (2017) Fatty acids in arbuscular mycorrhizal fungi are synthesized by the host plant. Science **356**: 1175–1178

Makarov MI (2019) The role of mycorrhiza in transformation of nitrogen compounds in soil and nitrogen nutrition of plants: a review. Eurasian Soil Sci **52**: 193–205

Marini AM, Soussi-Boudekou S, Vissers S, Andre B (1997) A family of ammonium transporters in *Saccharomyces cerevisiae*. Mol Cell Biol **17**: 4282–4293

McDonald TR, Dietrich FS, Lutzoni F (2012) Multiple horizontal gene transfers of ammonium transporters/ammonia permeases from prokaryotes to eukaryotes: toward a new functional and evolutionary classification. Mol Biol Evol **29**: 51–60

Miller RM, Miller SP, Jastrow JD, Rivetta CB (2002) Mycorrhizal mediated feedbacks influence net carbon gain and nutrient uptake in *Andropogon gerardii*. New Phytol **155**: 149–162

Nagy R, Vasconcelos MJ, Zhao S, McElver J, Bruce W, Amrhein N, Raghothama KG, Bucher M (2006) Differential regulation of five Pht1 phosphate transporters from maize (*Zea mays* L.). Plant Biol **8**: 186–197

Nelson DW, Sommers LE (1973) Determination of total nitrogen in plant material. Agron J **65**: 109–112

Neuhäuser B, Dynowski M, Ludewig U (2009) Channel-like NH_3 flux by ammonium transporter AtAMT2. FEBS Lett **583**: 2833–2838

Neuhäuser B, Dynowski M, Mayer M, Ludewig U (2007) Regulation of NH_4^+ transport by essential cross talk between AMT monomers through the carboxyl tails. Plant Physiol **143**: 1651–1659

Nouri E, Breuillin-Sessoms F, Feller U, Reinhardt D (2014) Phosphorus and nitrogen regulate arbuscular mycorrhizal symbiosis in *Petunia hybrida*. PLoS One **9**: e90841

Paszkowski U, Kroken S, Roux C, Briggs SP (2002) Rice phosphate transporters include an evolutionarily divergent gene specifically activated in arbuscular mycorrhizal symbiosis. Proc Natl Acad Sci USA **99**: 13324–13329

Peiffer JA, Spor A, Koren O, Jin Z, Tringe SG, Dangl JL, Buckler ES, Ley RE (2013) Diversity and heritability of the maize rhizosphere microbiome under field conditions. Proc Natl Acad Sci USA **110**: 6548–6553

Pérez-Tienda J, Testillano PS, Balestrini R, Fiorilli V, Azcon-Aguilar C, Ferrol N (2011) GintAMT2, a new member of the ammonium transporter family in the arbuscular mycorrhizal fungus *Glomus intraradices*. Fungal Genet Biol **48**: 1044–1055

Pfaffl MW (2001) A new mathematical model for relative quantification in real-time RT-PCR. Nucleic Acids Res **29**: e45

Pumplin N, Zhang X, Noar RD, Harrison MJ (2012) Polar localization of a symbiosis-specific phosphate transporter is mediated by a transient reorientation of secretion. Proc Natl Acad Sci USA **109**: E665–E672

Püschel D, Janoušková M, Hujslová M, Slavíková R, Gryndlerová H, Jansa J (2016) Plant-fungus competition for nitrogen erases mycorrhizal growth benefits of *Andropogon gerardii* under limited nitrogen supply. Ecol Evol **6**: 4332–4346

Reynolds HL, Hartley AE, Vogelsang KM, Bever JD, Schultz PA (2005) Arbuscular mycorrhizal fungi do not enhance nitrogen acquisition and growth of old-field perennials under low nitrogen supply in glasshouse culture. New Phytol **167**: 869–880

Ryan MH, Graham JH (2018) Little evidence that farmers should consider abundance or diversity of arbuscular mycorrhizal fungi when managing crops. New Phytol **220**: 1092–1107

Schalamuk S, Velazquez S, Chidichimo H, Cabello M (2004) Effect of no-till and conventional tillage on mycorrhizal colonization in spring wheat. Boletin Soc Argentina Bot **39**: 13–20

Smith SE, Read DJ (2008) Mycorrhizal Symbiosis. Academic Press, London

Smith SE, Smith FA (2011) Roles of arbuscular mycorrhizas in plant nutrition and growth: new paradigms from cellular to ecosystem scales. Annu Rev Plant Biol **62**: 227–250

Smith SE, Smith FA (2012) Fresh perspectives on the roles of arbuscular mycorrhizal fungi in plant nutrition and growth. Mycologia **104**: 1–13

Smith SE, Smith FA, Jakobsen I (2003) Mycorrhizal fungi can dominate phosphate supply to plants irrespective of growth responses. Plant Physiol **133**: 16–20

Smith SE, Smith FA, Jakobsen I (2004) Functional diversity in arbuscular mycorrhizal (AM) symbioses: the contribution of the mycorrhizal P uptake pathway is not correlated with mycorrhizal responses in growth or total P uptake. New Phytol **162**: 511–524

Smith SE, Jakobsen I, Gronlund M, Smith FA (2011) Roles of arbuscular mycorrhizas in plant phosphorus nutrition: interactions between pathways of phosphorus uptake in arbuscular mycorrhizal roots have important implications for understanding and manipulating plant phosphorus acquisition. Plant Physiol **156**: 1050–1057

Sohlenkamp C, Wood CC, Roeb GW, Udvardi MK (2002) Characterization of Arabidopsis AtAMT2, a high-affinity ammonium transporter of the plasma membrane. Plant Physiol **130**: 1788–1796

Straub D, Ludewig U, Neuhäuser B (2014) A nitrogen-dependent switch in the high affinity ammonium transport in *Medicago truncatula*. Plant Mol Biol **86**: 485–494

Tobar R, Azcon R, Barea JM (1994) Improved nitrogen uptake and transport from ^{15}N-labeled nitrate by external hyphae of arbuscular mycorrhiza under water-stressed conditions. New Phytol **126**: 119–122

Tanaka Y, Yano K (2005) Nitrogen delivery to maize via mycorrhizal hyphae depends on the form of N supplied. Plant Cell Environ **28**: 1247–1254

Tao K, Kelly S, Radutoiu S (2019) Microbial associations enabling nitrogen acquisition in plants. Curr Opin Microbiol **49**: 83–89

Thirkell TJ, Cameron DD, Hodge A (2016) Resolving the 'nitrogen paradox' of *arbuscular mycorrhizas*: fertilization with organic matter brings considerable benefits for plant nutrition and growth. Plant Cell Environ **39**: 1683–1690

Tian C, Kasiborski B, Koul R, Lammers PJ, Bücking H, Shachar-Hill Y (2010) Regulation of the nitrogen transfer pathway in the arbuscular mycorrhizal symbiosis: gene characterization and the coordination of expression with nitrogen flux. Plant Physiol **153**: 1175–1187

Trapnell C, Williams BA, Pertea G, Mortazavi A, Kwan G, van Baren MJ, Salzberg SL, Wold BJ, Pachter L (2010) Transcript assembly and quantification by RNA-Seq reveals unannotated transcripts and isoform switching during cell differentiation. Nat Biotechnol **28**: 511–515

Trouvelot A, Kough JL, Gianinazzi-Pearson V (1986) Mesure du taux de mycorhization VA d'un système radiculaire. Recherche des méthodes d'estimation ayant une signification fonctionnelle. *In* V Gianinazzi-Pearson, S Gianinazzi, eds, Physiological and Genetical Aspects of Mycorrhizae. Proceedings of the 1st European Symposium on Mycorrhizae, INRA Presse, Paris, pp 217–221

van der Heijden MG, Streitwolf-Engel R, Riedl R, Siegrist S, Neudecker A, Ineichen K, Boller T, Wiemken A, Sanders IR (2006) The mycorrhizal contribution to plant productivity, plant nutrition and soil structure in experimental grassland. New Phytol **172**: 739–752

Wang E, Yu N, Bano SA, Liu C, Miller AJ, Cousins D, Zhang X, Ratet P, Tadege M, Mysore KS, et al (2014) A H+-ATPase that energizes nutrient uptake during mycorrhizal symbioses in rice and Medicago truncatula. Plant Cell **26**: 1818–1830

Wang M, Chen C, Xu YY, Jiang RX, Han Y, Xu ZH, Chong K (2004) A practical vector for efficient knockdown of gene expression in rice (*Oryza sativa* L.). Plant Mol Biol Rep **22**: 409–417

Wang S, Chen A, Xie K, Yang X, Luo Z, Chen J, Zeng D, Ren Y, Yang C, Wang L, et al (2020) Functional analysis of the OsNPF4.5 nitrate transporter reveals a conserved mycorrhizal pathway of nitrogen acquisition in plants. Proc Natl Acad Sci USA **117**: 16649–16659

Wang W, Shi J, Xie Q, Jiang Y, Yu N, Wang E (2017) Nutrient exchange and regulation in arbuscular mycorrhizal symbiosis. Mol Plant **10**: 1147–1158

Wang XX, Wang X, Sun Y, Cheng Y, Liu S, Chen X, Feng G, Kuyper TW (2018) Arbuscular mycorrhizal fungi negatively affect nitrogen acquisition and grain yield of maize in a N deficient soil. Front Microbiol **9**: 418

Weidinger K, Neuhäuser B, Gilch S, Ludewig U, Meyer O, Schmidt I (2007) Functional and physiological evidence for a Rhesus-type ammonia transporter in *Nitrosomonas europaea*. FEMS Microbiol Lett **273**: 260–267

Williamson G, Tamburrino G, Bizior A, Boeckstaens M, Mirandela GD, Bage MG, Pisliakov A, Ives CM, Terras E, Hoskisson PA, et al (2020) A two-lane mechanism for selective biological ammonium transport. Elife **9**: e57183

Willmann M, Gerlach N, Buer B, Polatajko A, Nagy R, Koebke E, Jansa J, Flisch R, Bucher M (2013) Mycorrhizal phosphate uptake pathway in maize: vital for growth and cob development on nutrient poor agricultural and greenhouse soils. Front Plant Sci **4**: 533

Wu X, Liu T, Zhang Y, Duan F, Neuhäuser B, Ludewig U, Schulze WX, Yuan L (2019a) Ammonium and nitrate regulate NH_4^+ uptake activity of Arabidopsis ammonium transporter AtAMT1;3 via phosphorylation at multiple C-terminal sites. J Exp Bot **70**: 4919–4930

Wu XN, Xi L, Pertl-Obermeyer H, Li Z, Chu LC, Schulze WX (2017) Highly efficient single-step enrichment of low abundance phosphopeptides from plant membrane preparations. Front Plant Sci **8**: 1673

Wu XN, Chu LC, Xi L, Pertl-Obermeyer H, Li Z, Sklodowski K, Sanchez-Rodriguez C, Obermeyer G, Schulze WX (2019b) Sucrose-induced receptor kinase 1 is modulated by an interacting kinase with short extracellular domain. Mol Cell Proteomics **18**: 1556–1571

Xue L, Klinnawee L, Zhou Y, Saridis G, Vijayakumar V, Brands M, Dörmann P, Gigolashvili T, Turck F, Bucher M (2018) AP2 transcription factor CBX1 with a specific function in symbiotic exchange of nutrients in mycorrhizal *Lotus japonicus*. Proc Natl Acad Sci USA **115**: 9239–9246

Yang SY, Gronlund M, Jakobsen I, Grotemeyer MS, Rentsch D, Miyao A, Hirochika H, Kumar CS, Sundaresan V, Salamin N, et al (2012) Nonredundant regulation of rice arbuscular mycorrhizal symbiosis by two members of the *phosphate transporter1* gene family. Plant Cell **24**: 4236–4251

Yao Z, Zhang WS, Chen YX, Zhang W, Liu DY, Gao XP, Chen XP (2021) Nitrogen leaching and grey water footprint affected by nitrogen fertilization rate in maize production: a case study of southwest China. J Sci Food Agric. **101**: 6064–6073

Yoo SD, Cho YH, Sheen J (2007) *Arabidopsis* mesophyll protoplasts: a versatile cell system for transient gene expression analysis. Nat Protoc **2**: 1565–1572

Yuan L, Gu R, Xuan Y, Smith-Valle E, Loqué D, Frommer WB, von Wirén N (2013) Allosteric regulation of transport activity by heterotrimerization of *Arabidopsis* ammonium transporter complexes in vivo. Plant Cell **25**: 974–984

Zhang J, Liu YX, Zhang N, Hu B, Jin T, Xu H, Qin Y, Yan P, Zhang X, Guo X, et al (2019a) *NRT1.1B* is associated with root microbiota composition and nitrogen use in field-grown rice. Nat Biotechnol **37**: 676–684

Zhang S, Lehmann A, Zheng W, You Z, Rillig MC (2019b) Arbuscular mycorrhizal fungi increase grain yields: a meta-analysis. New Phytol **222**: 543–555

Zhang S, Wang L, Ma F, Bloomfield KJ, Yang J, Atkin OK (2015) Is resource allocation and grain yield of rice altered by inoculation with arbuscular mycorrhizal fungi? J Plant Ecol **8**: 436–448